CAPITAL UNIVERSITY OF SCIENCE AND
TECHNOLOGY, ISLAMABAD

Stability Analysis and Newton Basin of Attraction of Restricted Five Body Problem with Different Masses

by

Saman Israr

A thesis submitted in partial fulfillment for the
degree of Master of Philosophy

in the

Faculty of Computing
Department of Mathematics

2024

Dedicated to my parents especially my grandfather **M Banaras**, *who pray for me and always pave the way to success for me and my teachers*

CERTIFICATE OF APPROVAL

Stability Analysis and Newton Basin of Attraction of Restricted Five Body Problem with Different Masses

by

Saman Israr

(MMT213036)

THESIS EXAMINING COMMITTEE

(a)	External Examiner	Dr. Azad Akhter Siddiqui	NUST, Islamabad
(b)	Internal Examiner	Dr. Muhammad Afzal	CUST, Islamabad
(c)	Supervisor	Dr. Abdul Rehman Kashif	CUST, Islamabad

Dr. Abdul Rehman Kashif
Thesis Supervisor
June, 2024

Dr. Muhammad Sagheer
Head
Dept. of Mathematics
June, 2024

Dr. M. Abdul Qadir
Dean
Faculty of Computing
June, 2024

Author's Declaration

I, **Saman Israr** hereby state that my MPhil thesis titled "**Stability Analysis and Newton Basin of Attraction of Restricted Five Body Problem with Different Masses**" is my own work and has not been submitted previously by me for taking any degree from Capital University of Science and Technology, Islamabad or anywhere else in the country/abroad.

At any time if my statement is found to be incorrect even after my graduation, the University has the right to withdraw my MPhil Degree.

(Saman Israr)

Registration No: MMT213036

Plagiarism Undertaking

I solemnly declare that research work presented in this thesis titled "**Stability Analysis and Newton Basin of Attraction of Restricted Five Body Problem with Different Masses**" is solely my research work with no significant contribution from any other person. Small contribution/help wherever taken has been duly acknowledged and that complete thesis has been written by me.

I understand the zero tolerance policy of the HEC and Capital University of Science and Technology towards plagiarism. Therefore, I as an author of the above titled thesis declare that no portion of my thesis has been plagiarized and any material used as reference is properly referred/cited.

I undertake that if I am found guilty of any formal plagiarism in the above titled thesis even after award of MPhil Degree, the University reserves the right to withdraw/revoke my MPhil degree and that HEC and the University have the right to publish my name on the HEC/University website on which names of students are placed who submitted plagiarized work.

(Saman Israr)

Registration No: MMT213036

Acknowledgement

First and foremost I would like to pay my cordial gratitude to the almighty **Allah** who created us as a human being with the great boon of intellect. I would like to pay my humble gratitude to the Allah almighty, for blessing us with the holy prophet **Hazrat Mohammad (Sallallahu Alaihy Waalihi wassalam)** for whom the whole universe is being created. He (Sallallahu Alaihy Waalaihi wassalam) removed the ignorance from the society and brought us out of darkness. Thanks again to that Mono realistic power for granting me with a strength and courage whereby I delicately completed my MPhil thesis with positive and significant result. I owe honor, reverence and indebtedness to my accomplished supervisor and mentor **Dr. Abdul Rehman Kashif** whose affectionate guidance, authentic supervision, keen interest and ingenuity was a source of inspiration for commencement, advancement and completion of the present study. I would like to acknowledge CUST to provide me such a favorable environment to conduct this research. Thanks to parents, brother and my dear sister for their ever encouragement and overall support during my entire university life and my friends especially **Asma Amjad** for her support. May almighty Allah show his blessing and prosperity on all those who assisted me during the completion of this thesis.

(Saman Israr)

Registration No: MMT213036

Abstract

The first part of this thesis is a review of the central configuration of two cases discussed in article, Central configurations in the general four body coplanar problem with different masses. They identify the central configurations in the general coplanar four-body problem with four distinct masses. In this setup, three masses form a triangles vertices, while the fourth mass can be positioned elsewhere on the plane, forming either convex or concave central configurations. They establish the necessary conditions for the existence of central configurations and ensure the masses are positive. Using both analytical and numerical approaches, they found regions where central configurations are feasible. In the second part, we introduce a test mass, in the gravitational field of this central configuration. We analyze the motion of a fifth negligible mass without impacting the primary four-mass dynamics. By evaluating the fifth body equation of motion, we determine the equilibrium solution of the fifth mass. Additionally, we also investigate the Newton basins of attraction relative to these equilibrium points.

Contents

List of Figures

List of Tables

Abbreviations

CC	Central Configuration
CR3BP	Circular Restricted Three Body problem
2BP	Two Body Problem
3BP	Three Body Problem
R5BP	Restricted Five Body problem

Symbols

symbol	name	unit
$\mathbf{F}$	Gravitational Force	Newton
G	Universal Gravitational Constant	$m^3kg^{-1}s^{-2}$
d	Distance	Meter
$\mathbf{p}$	Linear Momentum	$kgms^{-1}$
$\mathbf{L}$	Angular Momentum	kgm^2s^{-1}
m_i	Point Mass	kg
$\wedge$	Cross Product	

Chapter 1

Introduction

1.1 Background

In mechanics, the n-body problem involves determining the individual movements of a collection of celestial objects influenced by gravitational interactions among themselves. The aim of addressing such problems is to understand the motion of celestial bodies like the moon, the sun, planets and visible stars. Mathematicians and astronomers in the 17th century were intrigued by the n-body problem. The problem statement asks, what will the orbit be if we have n celestial objects interacting with each other due to gravitational forces? Isaac Newton successfully tackled the two-body problem (2BP) using his laws of motion and the universal law of gravity. However, solving the problem for $n \geq 3$ has proven to be significantly challenging. Nonetheless, restricted versions of the n-body problem may offer specific solutions. Over the past four centuries, mathematicians and astronomers have persisted in their efforts to address the n-body problem. In the 17th century, Kepler work defined the elliptical paths of planets orbiting the sun in his planetary laws of motion published in **Philosophiae Naturalis Principia Mathematica** [1], a seminal work in scientific history. Isaac Newton formulation in this work derived and expounded upon Kepler laws, marking a crucial advancement in our understanding of celestial mechanics.

Roughly 67% of stars in our galaxy are believed to be part of multi-star systems, underscoring the significance of comprehending the four-body problem and the Restricted five-body problem. Central configurations are valuable tools for comprehending the gravitational dynamics inherent in n-body problems.

Central configurations within the n-body problem in a coplanar problem have been recognized for quite some time. These special equilibrium solutions involve a system of n bodies with masses (m_i) that rotate at a constant angular velocity around their center of mass. What makes central configurations (CC) noteworthy is that their geometric arrangement remains unchanged throughout their motion.

They possess a unique property in that they can be resized, repositioned, rotated or reflected, all while maintaining a consistent shape. Some well-known instances of central configurations include the five equilibrium solutions of Lagrange found in the Circular Restricted Three-Body Problem $(CR3BP)$, which result in three bodies arranged in a line at the L_1, L_2 and L_3 Lagrange points, as well as the two central configurations, each forming an equilateral triangle and originating from the L_4 and L_5 equilibrium points [2]. In the scenario of the equal-mass n-body problem, CC occur when a collection of n entities, all possessing identical mass are arranged at the vertices of an n-gon with uniform sides, expressed differently.

Additionally, solutions involving collinear formations of n bodies with equal mass arranged along a straight line have been established for quite some time [3]. Notably, the CC identified for the four-body equal mass problem include the square, equilateral triangle, concave kite, concave kite in the shape of an isosceles triangle, and four arrangements along a straight line as discussed by Palmore [4]. Moving towards the problem with unequal masses, the determination of central configurations becomes an algebraically challenging task, partic-ularly for $n \geq 4$. Simo [5] established the presence of relative equilibrium solutions within the general $4B$ problem, considering arbitrary masses for all four bodies. Furthermore, he derived the central configurations for a $(R4BP)$ involving three primary masses and one infinitesimal mass.

In 1998, Roy and Steves successfully derived Central configuration analyzed indirectly through an analytical approach for particular symmetric $4B$ problems characterized by two sets of equal masses organized symmetrically around an axis. They identified central configurations, such as the diamond-shapes convex kite, trapezoid, four collinear setup, and two triangular concave kites. Remarkably, these configurations were demonstrated to

converge to Lagrangian solutions as the mass of one set of masses approaches zero, ultimately reaching the limiting Circular Restricted Three-Body Problem ($CR3BP$). Shoaib [6] provided additional specifications for the central configurations of triangular concave kites.

Since then, numerous authors, including Albouy, Fu and Sun [7], Waldvogel [8], Erdi and Czirjak [9], Shoaib, et.al [10], Meyer and Schmidt [11], have dedicated their efforts to the examination of CC in the four-body problem. Their approach involves employing various symmetry restrictions to tackle the inherent complexity of the problem. A notable finding by Corbera, et.al. [12] established that any convex configuration of Four-bodies with diagonals of the quadrilateral at right angles to each other will invariably be a kite [2].

In a more general exploration, Erdi and Czirják [9] tackled a problem with one axis of symmetry, introducing angle coordinates to greatly simplify the derivation of CC for a range of convex and concave cases in the four-body problem ($4BP$). Alvarez and Llibre [13] contributed to this field by deriving central configurations specifically for Hjelmslev quadrilaterals and Equilic quadrilaterals. Equilic quadrilaterals are characterized by having two sides opposite each other inclined at a 60-degree angle, with equal lengths.

Waldvogel [8], Yan [14], Mello and Fernandes [15], and Perez-Chavela and Santoprete [16] have delved into the study of the four-body kite problem. In a related context, Bernat, et.al [17] focused on a $4B$ problem with three equal masses, providing an analysis that revealed the precise number of central configurations in the kite formation. In a different line of inquiry, Santoprete [18] explored a four-body problem characterized by a set of parallel sides. Employing distances as variables, they demonstrated the existence of central configurations in the form of isosceles trapezoids and kites.

Trapezoidal central configurations have been explored by various researchers, including Celli [19] and Corbera and Llibre [20]. Xia [21] provided a straightforward proof of the classical result established by MacMillan and Bartky [22]. In a more recent study by Corbera, et.al [23], they explored various types of trapezoids, such as those with equal sides (known as isosceles), those with acute angles, and those with a right angle. Additionally, they discussed how some trapezoids exhibit symmetry, meaning they look the same on both sides, while others lack this symmetry.

In their study, Cors and Roberts [24] di-rected their attention to co-circular trapezoidal CC. They found that these configurations

display a line of symmetry when two masses within the co-circular $4B$ CC are equal. Additionally, MacMillan and Bartky [22], apart from their research on quadrilaterals, also investigated isosceles trapezoidal configurations.

The exploration of symmetrical four-body CC contributes valuable insights to the broader understanding of four-body dynamics. This knowledge complements existing results, such as $3B$ and $4B$ equal mass CC, CC of convex kites, CC of concave kites, CC of trapezoids, and restricted cases involving three masses and a infinitesimal mass at their limits. These findings enhance our comprehension of both the general n-body and four-body problems.

Researchers have extensively studied the stability of these CC through numerical and analytical approaches, as demonstrated by the works of Bakker and Simmons [25] and Yan [14]. The analysis of CC provides valuable insights into periodic orbits, stability, and refinement points within the broader context of n-body and $4B$ problems.

In a News and Reviews article in Nature [26], reviewing advancements in $4B$ CC, Hamilton [27] highlighted in his result the potential significance of symmetrical four-body CC. He suggested that these configurations could potentially be utilized as boundary cases for ambitious future expansions of the n-body problem. For instance, these symmetrical configurations might offer insights into scenarios such as m_1, m_2, m_3 along a line with two symmetrically placed equal masses, configurations involving a test particle with planar arrangements similar to those studied in the present work, or even planar setups featuring four masses of different magnitudes.
This perspective underscores the ongoing exploration and potential applications of symmetrical four-body CC in advancing our understanding of celestial dynamics. These findings could potentially serve as foundational scenarios for ambitious expansions of the n-body problem in the future.

For instance, they might include scenarios such as three masses aligned on a line with two equally positioned equal masses, a test particle alongside planar configurations similar to those explored in the current study, or even planar arrangements involving four distinct masses.

Newton's Basins of Attraction

The Newton-Raphson iterative scheme identifies convergence basins associated with Lagrange points by utilizing intrinsic properties of dynamic systems. Existing literature

investigate into these basins across various dynamic systems, including the restricted three-body problem [28, 29]. In a recent study, Suraj et al. explored the analysis of the $R5BP$ within the frame of variable mass examining Lagrange point location, movement, and stability concerning a perturbation parameter influenced by the variable mass of a fifth small body [30]. They employed the iterative Newton-Raphson bivariate scheme to investigate convergence basins for equilibrium points. These basins of attraction illustrate how the system equilibrium points attract initial conditions, forming nodes on the configuration plane, constituting the convergence domain. Newton-Raphson convergence basins, linked to Lagrange points operating as attractors, were discussed in the planar circular restricted five-body problem [31]. Other studies, such as Bogdan et.al., discussed attraction fractal basins associated with the damped Newton approach [32]. Suraj et al. also recently studied concave axisymmetric configurations in numerically restricted five-body problems, using the iterative Newton-Raphson scheme to analyze convergence basins [33].

Thesis Contribution

The first section of this thesis reviews two cases discussed in [2] concerning the central configuration. These cases analyze the general coplanar four-body problem with four distinct masses. In this scenario, three masses form the vertices of a triangle, while the fourth mass can be positioned elsewhere on the plane, resulting in either convex or concave central configurations. The authors establish the necessary conditions for the existence of CC and ensure that the masses are positive. Using both analytical and numerical methods, they identify feasible regions for central configurations. In the second section, we introduce a test mass into the gravitational field of this central configuration. We examine the motion of a fifth negligible mass without affecting the primary dynamics of the four-mass system. By evaluating the equation of motion for the fifth body, we determine its equilibrium solution. Additionally, we investigate the Newton basins of attraction relative to these equilibrium points.

Chapter 2

Preliminaries

In this chapter, we will give core definitions, fundamental concepts, universal principles, and laws that contribute to a deeper understanding of our research efforts.

2.1 Basic Definitions

2.1.1 Celestial Mechanics [34]

"Celestial mechanics is the branch of astronomy that deals with the motions of objects in outer space. Historically, celestial mechanics applies principles of physics (classical mechanics) to astronomical objects, such as stars and planets, to produce ephemeris data.

2.1.2 Vector [34]

"The quantities of physics, such as displacement, velocity, momentum, force etc require for their specification a direction as well as magnitude. Such quantities are called **Vectors**."

2.1.3 Scalar [34]

"Various quantities of physics, such as length, mass and time, requires for their specification a single real number (apart from units of measurement which are decided upon in advance).

Such quantities are called **Scalars** and the real number is called the magnitude of the quantity".

2.1.4 Field [34]

"A field is a physical quantity associated with every point of space time. The physical quantity may be either in vector form, scalar form or tensor form."

2.1.5 Scalar Field [34]

"If at every point in a region, a scalar function has a defined value, the region is called a scalar field,
e.g. temperature and pressure fields around the earth."

2.1.6 Vector Field [34]

"If at every point in a region, a vector function has a defined value, the region is called a vector field,
e.g. tangent vector around a smooth curve."

2.1.7 Conservative Vector Field [34]

"A vector field $\mathbf{V}$ is conservative if and only if there exists a continuously differentiable scalar field f such that $\mathbf{V} = \nabla f$ or equivalently if and only if

$$\nabla \times \mathbf{V} = Curl\, \mathbf{V} = 0."$$

2.1.8 Uniform Force Field [34]

"A force field which has constant magnitude and direction is called a uniform or constant force field. If the direction of the field is taken as negative z direction and magnitude is constant $F_0 > 0$, then the force field is given by

$$\mathbf{F} = -F_0\hat{\mathbf{k}}."$$

2.1.9 Central Force Field [35]

"A force is said to be central under two conditions. First, the direction of the force must always be towards or away from fixed point. The point is known as the center of force.

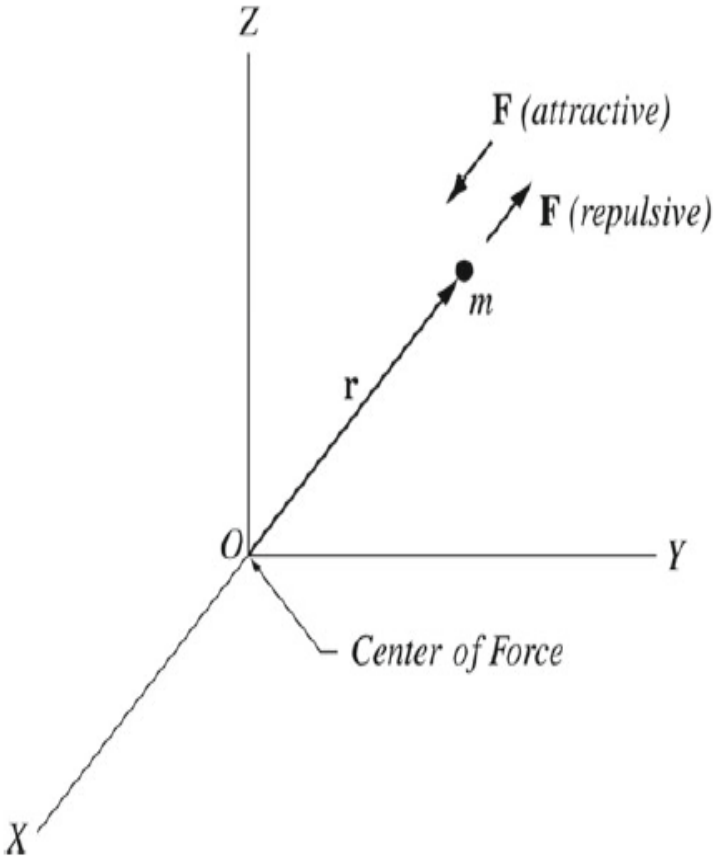

FIGURE 2.1: The central force

Second, the magnitude of the force should only proportional to the distance **r** between the particle and center of the force. The central force may be written as

$$\mathbf{F} = f(r)\mathbf{r}_1,$$

where $\mathbf{r}_1$ is a unit vector in the direction of $\mathbf{r}$. Therefore, if $f(r) < 0$, then the central force is an attractive force since it is directed toward the center of the force $\mathbf{O}$ and if $f(r) > 0$, the force is repulsively directed away from $\mathbf{O}$.
The most widely known are the gravitational force and Coulomb force."

2.1.10 Degree of Freedom [34]

"The number of coordinates required to specify the position of a system of one or more particles is called number of degree of freedom of the system.

Example: A particle moving freely in space requires 3 coordinates, e.g. x, y, z, to specify its position. Thus the number of degree of freedom is 3."

2.1.11 Central Configuration [36]

"A central configuration is a special arrangement of point masses interacting by Newton's law of gravitation with the following property: the gravitational acceleration vector produced on each mass by all the others should point toward the center of mass and be proportional to the distance to the center of mass."

2.1.12 Center of Mass [34]

"Let $\mathbf{r_1}, \mathbf{r_2}, ..., \mathbf{r_n}$ be the position vector of a system of n particles of masses $m_1, m_2, ...m_n$ respectively. The center of mass or centroid of the system of particlesis defined as that point having position vector

$$\hat{\mathbf{r}} = \frac{m_1\mathbf{r}_1 + m_2\mathbf{r}_2 + ... + m_n\mathbf{r}_n}{m_1 + m_2 + ... + m_n},$$

$$= \frac{1}{\mathbf{M}} \sum_{v=1}^{n} m_v \mathbf{r}_v,$$

where

$$\mathbf{M} = \sum_{v=1}^{n} m_v,$$

is the total mass of the system."

2.1.13 Torque [35]

"The torque is a vector quantity that measures the tendency of that force to rotate the particle about O and is defined as

$$\boldsymbol{\tau} = \mathbf{r} \times \mathbf{F}.$$

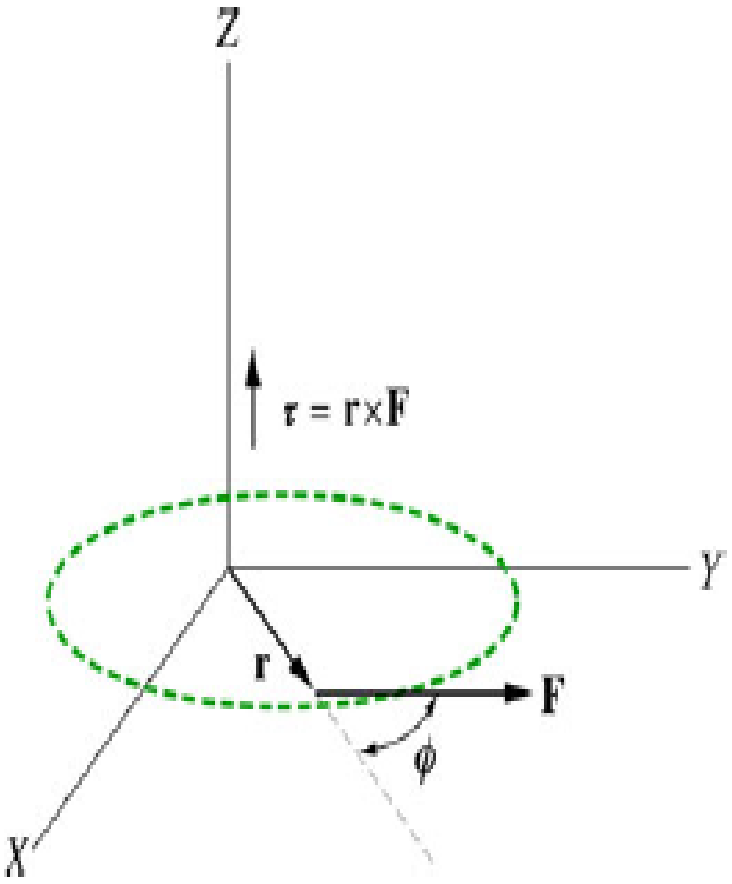

FIGURE 2.2: A particle in the $x-y$ plane exposed to a force that lies in that plane. The resulting torque is then perpendicular to the $x-y$ plane parallel to the z-axis

The direction of $\boldsymbol{\tau}$ is perpendicular to the plane formed by $\mathbf{r}$ and $\mathbf{F}$. From the vector product definition, this quantity has a magnitude given by

$$\tau = rFsin\phi.$$

where ϕ is the smaller angle between r and F, τ is positive if the force tends to rotate the particle counter-clockwise and negative if it tends to rotate it clockwise."

2.1.14 Momentum [35]

"The linear momentum (or quantity of motion as was called by Newton) of a particle of mass m is a vector quantity defined as

$$\mathbf{p} = m\mathbf{v}.$$

where $\mathbf{v}$ is the velocity of the particle. A fast moving car has more momentum than a slow moving car of the same mass. Newton's second law can be expressed in terms of momentum for a particle-like object of constant mass as

$$\sum \mathbf{F} = m\mathbf{a} = m\frac{d\mathbf{v}}{dt} = \frac{d(m\mathbf{v})}{dt},$$

or

$$\sum \mathbf{F} = \frac{d\mathbf{p}}{dt},$$

that is, the rate of change of the linear momentum of an object is equal to the resultant force acting on the object and is in the same direction as that of force."

2.1.15 Conservation of Linear Momentum [35]

"If the net external force on a system is zero, the total linear momentum of the system remains unchanged, i-e

$$\mathbf{p}_{tot} = \mathbf{p}_1 + \mathbf{p}_2$$

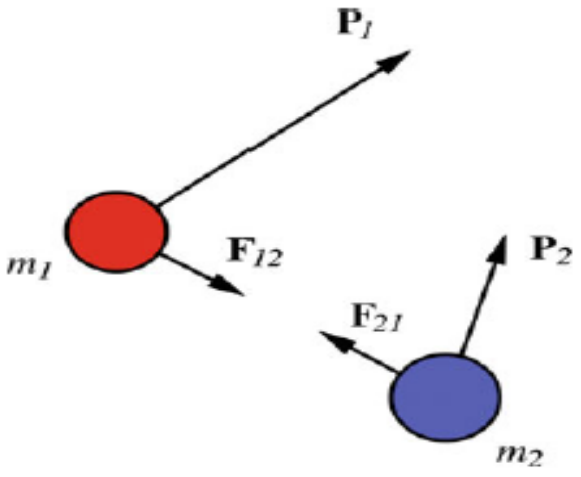

FIGURE 2.3: An isolated system consisting of two particles where the only forces that act in the system are internal forces

$$\mathbf{F}_{12} = -\mathbf{F}_{21}$$

where $\mathbf{F_{12}}$ is a force exerted on particle 2 by particle 1, then by Newton's third law of motion $\mathbf{F_{21}}$ is a force exerted on particle 1 by particle 2.

$$\frac{d\mathbf{p}_{tot}}{dt} = \frac{d\mathbf{p}_1}{dt} + \frac{d\mathbf{p}_2}{dt} = \mathbf{F}_{12} + \mathbf{F}_{21} = \mathbf{F}_{12} - \mathbf{F}_{12} = 0,$$

$$\mathbf{p} = C,$$

where C is constant. Thus,

$$\mathbf{p}_i = \mathbf{p}_f.$$"

2.1.16 Point like Particle [34]

"A point-like particle is an idealization of particles mostly used in different fi elds of physics. Its defining features is the lacks of spatial extension: being zero-dimensional, it does not take up space.

A point-like particle is an appropriate representation of an object whose structure, size and shape is irrelevant in a given context. e.g., from far away, a finite-size mass (object) will look like a point-like particle."

2.1.17 Angular Momentum [35]

"The angular momentum $\mathbf{L}$ of a particle of mass m and linear momentum $\mathbf{p}$ is a vector quantity defined as:

$$\mathbf{L} = \mathbf{r} \times \mathbf{p},$$

where $\mathbf{r}$ is the position vector of the particle relative to an origin O that is in an inertial frame and $\mathbf{p}$ is the linear momentum. From the definition of torque, we have

$$\boldsymbol{\tau} = \frac{d\mathbf{L}}{dt}. \tag{2.1}$$

This implies that the torque acting on a particle is equal to the time rate of change of the angular momentum for that particle. This equation is valid only if $\boldsymbol{\tau}$ and $\mathbf{L}$ are evaluated with respect to the same origin or any other fixed point in an inertial frame."

2.1.18 Conservation of Angular Momentum [35]

"The total angular momentum of a particle is constant if the net external torque acting on it is zero:

$$\sum \boldsymbol{\tau_{ext}} = \frac{d\mathbf{L}}{dt} = 0,$$

$$\mathbf{L} = C,$$

where C is constant.

$$\mathbf{L}_i = \mathbf{L}_f."$$

2.1.18.1 Inertial Frame of Reference

"A frame of reference that remains at rest or moves with constant velocity with respect to other frames of reference is called inertial frame of reference. Actually, an unaccelerated frame of reference is an inertial frame of reference.

In this frame of reference a body does not acted upon by external forces. Newton's laws of motion are valid in all inertial frames of reference. All inertial frames of reference are equivalent"

2.1.18.2 Non-Inertial Frame of Reference

"A non-inertial reference frame is a frame of reference that is undergoing acceleration with respect to an inertial frame.
The the laws of motion are the same in all inertial frames and in non-inertial frames, they vary from frame to frame depending on the acceleration."

2.1.19 Equilibrium Solution [34]

"The equilibrium solution can guide us through the behaviour of the equation that represents the problem without actually solving it. These solutions can be found only if we

meet the sufficient condition of all rates equal to zero. If we have two variables then

$$\dot{x} = \dot{y} = \ddot{x} = \ddot{y} = ... = x^n = y^n = 0.$$

These solutions may be stable or unstable. The stable solutions regarding in celestial Mechanics helps us find parking spaces where if a satellite or any object placed, it will remain there for ever. These type of places are also found along the Jupiter's orbital path where bodies called trojan are present.

These equilibrium points with respect to Celestial Mechanics are also called Lagrange points named after a French mathematician and astronomer Joseph-Louis Lagrange. He was first to find these equilibrium points for the Sun-Earth system. He found that three of these five points were collinear."

2.1.20 Lagrange Points [34]

"A point in space where a small body with negligible mass under the gravitational influence of four large bodies will remain at rest relative to the larger ones.

These points are locations in an orbital arrangement of two large bodies where a third smaller body, affected solely by gravity, is capable of maintaining a stable position relative to the two larger bodies.

A Lagrange point is also known as a equilibrium point or Liberation point named after a French mathematician and astronomer Joseph-Louis Lagrange. He was first to find these equilibrium points for the earth, sun, and moon system. He found five points out of these three are collinear."

2.1.21 Basin of Attraction [34]

"Newton method is used to find the roots of equations but Arthur Cayley found that if the roots of a function are already know then Newton's method can guide to another problem that is which initial guesses iterate to which roots and the region of these initial guesses is called basins of attraction of the roots."

2.1.22 Keplers Laws [35]

"After analyzing the astronomical data of the Danish astronomer Tycho Brahe, the German astronomer Johannes Kepler formulated his three laws of planetary motion

2.1.22.1 Keplers First Law [35]

Every planet moves in an elliptical orbit with the sun at one focus.

2.1.22.2 Keplers Second Law [35]

The radius vector drawn from the sun to the planet sweeps out equal areas in equal periods of time.

2.1.22.3 Keplers Third Law [35]

The square of the period of revolution of any planet about the sun is proportional to the cube of the semimajor axis of its orbit.

$$T^2 = \left(\frac{4\pi^2}{GM_s}\right) a^3.$$

where T is the time period, a is the semi major axis, M_s is the mass of sun and G is the universal gravitational constant."

2.1.23 Procedure for Stability Analysis and Equilibrium Points [34]

"Stability analysis is the examination of a system or solution tendency to maintain its equilibrium or return to it after experiencing perturbations or disturbances." We can check the stability of equilibrium points by following these steps.

1. "Determine the equilibrium points, x^*, solving $\Omega\ (x^*) = 0$, where $\Omega\ (x^*)$ is effective potential.

2. Construct the Jacobian matrix, $J(x^*) = \dfrac{d\Omega}{dx}$.
3. Compute eigenvalues of $\Omega(x^*)$: $\det|\Omega(x^*) - \lambda I| = 0$

4. Stability or instability of x^* based on the real parts of eigenvalues.

5. Point is stable, if all eigenvalues have real parts negative.

6. Unstable, if at least one of the eigenvalues have a real part greater than zero.

7. Otherwise, there is no conclusion, (i.e, require an investigation of higher order terms)."

2.1.24 Newtons Laws of Motion [35]

"Sir Isaac Newton (1642-1727) formulated his three famous laws of motion describing the relationship between the force acting on an object and the acceleration of that object. Newtonian or classical mechanics which is based mainly on Newton's three laws of motion are:

1. First Law of Motion An object at rest remains at rest and an object in motion will continue in motion with constant velocity (constant speed in a straight line) unless acted upon by a net external force, i-e

$$\sum \mathbf{F} = 0,$$

$$\Rightarrow \mathbf{a} = 0.$$

2. Second Law of Motion The acceleration of an object produced by a net external force is directly proportional to the force in a direction parallel to that force and is inversely proportional to its mass, that is,

$$\sum \mathbf{F} = m\mathbf{a}.$$

where $\mathbf{a}$ is acceleration and m is mass of object.

3. Third Law of Motion To every action there is an equal and opposite reaction."

2.1.25 Newtons Universal Law of Gravitation [34]

"Every particle of matter in the universe attracts every other particle of matter with a force which is directly proportional to the product of the masses and inversely proportional to the square of the distance between them. Hence, for any two particles separated by a distance r, the magnitude of the gravitational force $\mathbf{F}$ is:

$$\mathbf{F} = G\frac{m_1 m_2}{r^3}\mathbf{r}.$$

where G is universal gravitational constant and m_1 and m_2 are the masses of the particles respectively. Its numerical value in SI units is $6.67408 \times 10^{-11} m^3 kg^{-1} s^{-2}$."

2.2 Two Body Problem [37]

"The two-body problem, first studied and resolved by Newton, states: Suppose that at time t the positions and velocities of two celestial bodies moving under their mutual gravitational force, then what should be their location and velocity at any other time, if the masses are known."

1. In celestial mechanics, it is the only gravity problem for which closed form solution is known.

2. A large scope of realistic elliptic motion issues can be viewed as approximately $2BP$.

3. In order to provide approximate orbital parameters and forecasts, the two body solution may be used as a initial point for producing analytical solutions that are accurate for higher precision orders.

2.3 The Solution to the Two-Body Problem [38]

"Newton's universal gravitational law is the governing law for the two bodies:

$$\mathbf{F} = G\frac{m_1 m_2}{d^3}\mathbf{d}, \tag{2.2}$$

for two masses, m_1 and m_2 are separated by a d distance, and the universal gravitational constant is **G**."

The objective is to determine the trajectory of particles over a given time t when we have information about their initial positions and velocities. In Figure (2.2), the force of attraction $\mathbf{F}_{12}$ acts in the direction of m_1 along the vector $\mathbf{d}$, while the force $\mathbf{F}_{21}$ on m_2 acts in the opposite direction. This situation adheres to Newton's third law of motion, which states that for every action, there is an equal and opposite reaction, i-e,

$$\boldsymbol{F_{12} = -F_{21}.} \tag{2.3}$$

From figure 2.4, Newton's second law is described by equations (2.2) and (2.3) when applied to particles under the influence of gravity, with equations (2.2) and (2.3) specifying their respective contributions as follows,

$$m\ddot{\mathbf{d}} = G\frac{m_1 m_2}{d^3}\mathbf{d}, \tag{2.4}$$

$$m_2\ddot{\mathbf{d_1}} = G\frac{m_1 m_2}{d^3}\mathbf{d}, \tag{2.5}$$

and,

$$m_2\ddot{\mathbf{d_2}} = -G\frac{m_1 m_2}{d^3}\mathbf{d}. \tag{2.6}$$

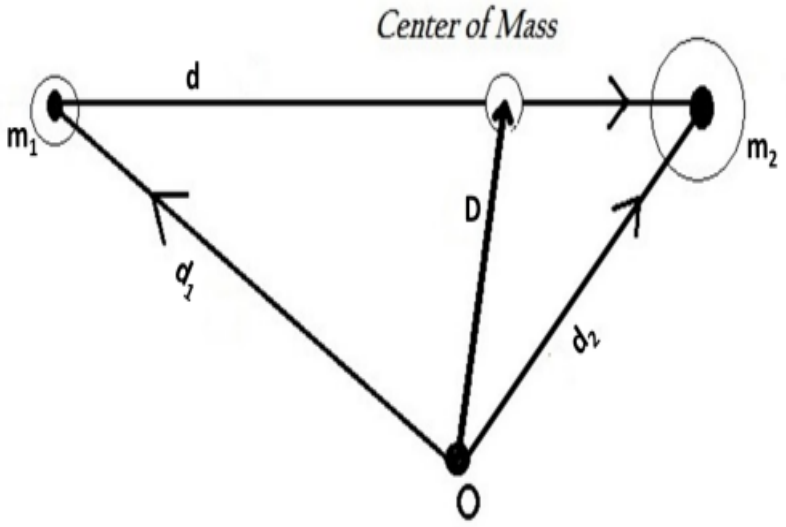

FIGURE 2.4: Center of Mass.

Adding equations (2.5) and (2.6), we derive the following results, taking into account the location vectors $\mathbf{d}_1$ and $\mathbf{d}_2$ with respect to the reference point O, as depicted in figure

2.4.

$$m_1\ddot{\mathbf{d_1}} + m_2\ddot{\mathbf{d_2}} = 0. \tag{2.7}$$

Integrating above equation, we get

$$m_1\dot{\mathbf{d_1}} + m_2\dot{\mathbf{d_2}} = \mathbf{k_1}, \tag{2.8}$$

where $\mathbf{k_1}$ is the constant of integration.
The system maintains a constant total linear momentum, in other words: $m_1\mathbf{v_{m_1}} + m_2\mathbf{v_{m_2}} = \mathbf{k_1}$. Integrating equation (2.8) once more leads to the following result:

$$m_1\mathbf{d_1} + m_2\mathbf{d_2} = \mathbf{k_1}t + \mathbf{k_2}, \tag{2.9}$$

if $\mathbf{D}$ is the center of mass of masses m_1 and m_2 then from the definition of center of mass, we can write as:

$$m_t\mathbf{D} = m_1\mathbf{d_1} + m_2\mathbf{d_2}, \tag{2.10}$$

where m_t is sum of masses m_1 and m_2. Differentiating equation (2.10) and then compare with equation (2.8), we see

$$m_t\dot{\mathbf{D}} = \mathbf{k_1} \implies \dot{\mathbf{D}} = \frac{\mathbf{k_1}}{m_t} = Constant.$$

The velocity of center of mass is constant.

By subtracting equation (2.7) from equation (2.6)

$$\ddot{\mathbf{d_1}} - \ddot{\mathbf{d_2}} = G\frac{m_2}{d^3}\mathbf{d} + G\frac{m_1}{d^3}\mathbf{d}, \tag{2.11}$$

$$\Rightarrow \ddot{\mathbf{d_1}} - \ddot{\mathbf{d_2}} = G(m_2 + m_1)\frac{\mathbf{d}}{d^3}.$$

$$\Rightarrow \ddot{\mathbf{d}} = \beta\frac{\mathbf{d}}{d^3},$$

$$\implies \ddot{\mathbf{d}} + \beta\frac{\mathbf{d}}{d^3} = 0, \tag{2.12}$$

where $\beta = G(m_1 + m_2)$ which is the reduced mass and $\mathbf{d_1} - \mathbf{d_2} = \mathbf{d}$ which is shown in figure 2.4.

Now we multiply $\mathbf{d}$ with equation (2.12),

$$\mathbf{d} \times \beta \ddot{\mathbf{d}} + \frac{\beta^2}{d^3} \mathbf{d} \times \mathbf{d} = 0,$$

$$\implies \mathbf{d} \times \ddot{\mathbf{d}} = 0. \tag{2.13}$$

By integrating above equation becomes:

$$\mathbf{d} \times \dot{\mathbf{d}} = \mathbf{H}, \tag{2.14}$$

where $\mathbf{H}$ is integration constant.

Equation (2.12) becomes,

$$\implies \mathbf{d} \times \beta \ddot{\mathbf{d}} = 0, \tag{2.15}$$

$$\implies \mathbf{d} \times \mathbf{F} = 0, \tag{2.16}$$

where by comparing equation (2.15) and (2.16),

$$\mathbf{F} = \beta \ddot{\mathbf{d}}.$$

The relationship between torque and angular momentum is given as follow,

$$\boldsymbol{\tau} = \mathbf{d} \times \mathbf{F}. \tag{2.17}$$

By comparing equation (2.16) and (2.17),

$$\boldsymbol{\tau} = \mathbf{d} \times \mathbf{F} = 0, \tag{2.18}$$

by comparing equation (2.1) and (2.18),

$$\Rightarrow \frac{d\mathbf{L}}{dt} = 0, \tag{2.19}$$

$$\mathbf{L} = \mathbf{C}.$$

This implies that angular momentum $\mathbf{L}$ remains constant or is conserved.

2.4 Velocity and Acceleration Components of Radial and Transverse

If we select polar coordinates d and θ within this depicted region, the velocity components along and perpendicular to the radius vector connecting m_1 and m_2 are represented as $\dot{d}$ and $d\dot{\theta}$, as illustrated in figure 2.5.

$$\mathbf{v} = \dot{\mathbf{d}} = \dot{\mathbf{d}}\mathbf{i} + \mathbf{d}\dot{\theta}\mathbf{j}. \tag{2.20}$$

Where $\mathbf{v}$ is the velocity of particle in polar coordinate and unit vectors $\mathbf{i}$ and $\mathbf{j}$ are positioned parallel and perpendicular to the radius vector. Taking cross product with $d\mathbf{i}$,

$$d\mathbf{i} \times (\dot{d}\mathbf{i} + d\dot{\theta}\mathbf{j}) = d^2\dot{\theta}\mathbf{k} = \mathbf{L}\mathbf{k}, \tag{2.21}$$

the unit vector $\mathbf{k}$ is orthogonal or perpendicular to the orbital plane. We can write,

$$d^2\dot{\theta} = \mathbf{L}, \tag{2.22}$$

since $\mathbf{L}$ remains constant and is demonstrated to be twice the rate of change of the radius vector, this provides a mathematical representation of Kepler's second law. From figure(2.4) we know that $\dot{\mathbf{d_1}} - \dot{\mathbf{d_2}} = -\dot{\mathbf{d}}$ so we can write equation (2.4) as $\frac{d^2(-\dot{\mathbf{d}})}{dt^2} = G\frac{m_1 m_2}{d^3}\mathbf{d}$ where $G(m_1 + m_2)$ are constant so,

$$\frac{d^2(\dot{\mathbf{d}})}{dt^2} + \beta\frac{\mathbf{d}}{d^3}\mathbf{d} = 0, \tag{2.23}$$

if we take the dot product of $\dot{\mathbf{d}}$ with equation (2.23) we derive the following equations, as shown below.

$$\dot{\mathbf{d}} \cdot \frac{d^2\mathbf{d}}{dt^2} + \beta\frac{\dot{\mathbf{d}} \cdot \mathbf{d}}{d^3} = 0.$$

After integrating the above equation we get,

$$\frac{1}{2}\dot{\mathbf{d}} \cdot \dot{\mathbf{d}} - \frac{\beta}{d} = H, \tag{2.24}$$

$$\frac{1}{2}v^2 - \frac{\beta}{d} = H. \tag{2.25}$$

The constant H represents energy conservation in this system. It's important to note that H does not represent the absolute energy; instead, $\frac{1}{2}v^2$ corresponds to kinetic energy (KE), and $\frac{-\beta}{d}$ corresponds to potential energy (PE) of the system. This means that the total energy of the system remains constant. When considering the elements of the acceleration vector in celestial mechanics, the radius vector is both perpendicular to and aligned along certain directions.

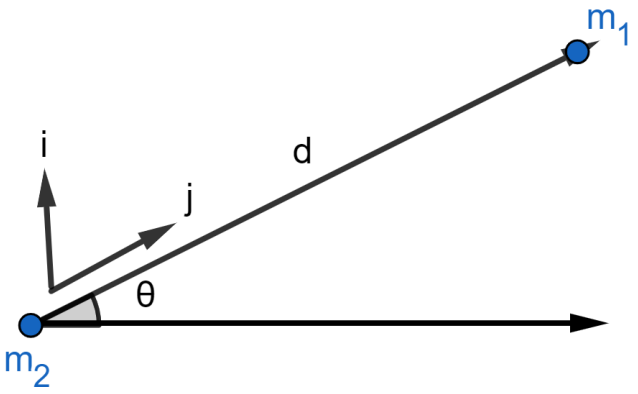

FIGURE 2.5: Radial and transverse components of velocity and acceleration

Taking the derivative of equation (2.20), the acceleration vector is given as follows

$$\mathbf{a} = (\ddot{d} - d\dot{\theta}^2)\mathbf{i} + \frac{1}{d}\frac{d}{dt}(d^2\theta)\mathbf{j}, \tag{2.26}$$

above equation is used in equation(2.23), we obtain,

$$\ddot{d} - d\dot{\theta}^2 = -\frac{\beta}{d^2}, \tag{2.27}$$

$$\frac{1}{d}\frac{d}{dt}(d^2\dot{\theta}) = 0. \tag{2.28}$$

Following further integration of equation (2.28), we arrive at the subsequent integral for angular momentum.

$$d^2\dot{\theta} = \mathbf{L}. \tag{2.29}$$

With this type of substitution,

$$u = \frac{1}{d}, \tag{2.30}$$

by using equation (2.30) in central force we get:

$$\frac{d^2u}{d\theta^2} + u = \frac{\beta}{L^2}, \tag{2.31}$$

the equation above exhibits a familiar shape, which is:

$$u = \frac{\beta}{L^2} + B\cos(\theta - \theta_0), \tag{2.32}$$

in the given equation, substitute $u = \frac{1}{d}$, where B and θ_0 are integration constants.

$$\frac{1}{d} = \frac{\beta}{L^2} + B\cos(\theta - \theta_0), \tag{2.33}$$

$$d = \frac{\frac{\beta}{L^2}}{1 + \frac{L^2 B_1}{\beta}\cos(\theta - \theta_0)},$$

the polar form of the conical equation can be expressed as:

$$d = \frac{p}{1 + \epsilon\cos(\theta - \theta_0)},$$

where

$$p = \frac{L^2}{\beta},$$

$$\epsilon = \frac{BL^2}{\beta}.$$

The trajectory of one celestial body as it revolves around another is characterized by the eccentricity (ϵ) of the orbit, and it can be classified as follows:

1 The orbit is elliptical if $0 < \epsilon < 1$.

2 The orbit is parabolic if $\epsilon = 1$.

3 Likewise, the orbit is hyperbolic if $\epsilon > 1$.

Consequently, a conic shape serves as the solution to the two-body problem ($2BP$), and this includes the first law of Kepler as a particular instance. In mathematical terms, it can be expressed as follows.

$$\epsilon = \frac{c}{a}.$$

"c" denotes the distance from the focus to the center.

"a" represents the semi-major axis.

"b" represents the semi-minor axis.

These parameters are commonly used in the description of conic sections and are essential for understanding their properties and shapes.

$$a^2 = b^2 + c^2,$$

$$c^2 = a^2 - b^2.$$

2.5 Three Body Problem

"In the three-body problem, three bodies move in space under their mutual gravitational interactions as described by Newton's theory of gravity. Solutions of this problem require that future and past motions of the bodies be uniquely determined based solely on their present positions and velocities. In general, the motions of the bodies take place in three dimensions (3D), and there are no restrictions on their masses nor on the initial conditions. Thus, we refer to this as the general three-body problem".

Chapter 3

Central Configurations in the Coplanar Four-Body Problem with Varying Masses

3.1 Introduction

In this review work of research, we will focus on a detailed discussion of two cases of central configuration of a general four-body problem discussed in [2]. They established the essential criteria for the presence of central configurations involving four bodies. Additionally, they outlined the formulas for mass ratios and identified the equations that establish the boundaries within which each mass ratio is positive.

These four bodies possess distinct masses, are situated in the same plane, but are not aligned in a straight line.

3.1.1 The Equations for Central Configurations

We examine a scenario involving four point masses, denoted as m_i, with position vectors $\mathbf{r_i}$ and the distances between them, r_{ij}, where i and j can take values of $0-3$.
It is important to note that these masses lie within the same plane but are not positioned

in a straight line. The equations for a central configuration that is not collinear can be formulated as follows [2];

$$f_{ij} = \sum_{k=0,k\neq i,j}^{n-1} m_k(S_{ik} - S_{jk})\Delta_{ijk} = 0, \tag{3.1}$$

where

$$S_{ij} = r_{ij}^{-3} \text{ and } \Delta_{ijk} = (r_i - r_j) \wedge (r_i - r_k),$$

and the quantity Δ_{ijk} represent the area determined by $(r_i - r_j)$ and $(r_i - r_k)$. We observe that a central configuration maintains its essential properties when subjected to operations like scaling, translation, rotation, or reflection. Utilizing this invariance, we can streamline our analysis without sacrificing generality.

Assuming none of the masses overlap, begin by selecting one of the mass which we will call m_1, and position it at the coordinates $\mathbf{r_1} = (-1, 0)$. Then, choose two other masses, m_0 and m_2 and adjust the entire system orientation through rotation so that the line connecting m_0 and m_2 becomes perpendicular to the x-axis. While preserving the position of m_1 and the orientation of the system, uniformly scale the entire configuration until m_0 and m_2 align with the y-axis. If necessary, to simplify the analysis without losing generality, we can mirror the system across the x-axis, ensuring that m_0 is located at $\mathbf{r_0} = (0, b)$ and m_2 is positioned at $\mathbf{r_2} = (0, a)$, with $b < a$.

Lastly, designate the coordinates of the final mass m_3, as $\mathbf{r_3} = (c_1, c_2)$. With these adjustments made, we can then express the quantities S_{ij} and Δ_{ijk} as required.

$$\left.\begin{aligned} S_{01} = \frac{1}{\varsigma},\ S_{02} = \frac{1}{\tau},\ S_{12} = \frac{1}{\sigma}, \\ S_{03} = \frac{1}{T},\ S_{13} = \frac{1}{M},\ S_{23} = \frac{1}{G}, \end{aligned}\right\} \tag{3.2}$$

$$\left.\begin{aligned} \Delta_{012} = b - a,\ \Delta_{013} = b + bc_1 - c_2, \\ \Delta_{023} = (b - a)c_1,\ \Delta_{123} = c_2 - a - ac_1, \end{aligned}\right\} \tag{3.3}$$

where

$$\sigma = (1+a^2)^{\frac{3}{2}},\ \varsigma = (1+b^2)^{\frac{3}{2}},\ \tau = (a-b)^3,$$

$$G = (c_1^2 + (c_2-a)^2)^{\frac{3}{2}},\ T = (c_1^2 + (c_2-b)^2)^{\frac{3}{2}},\ M = (c_2^2 + (c_1+1)^2)^{\frac{3}{2}}.$$

Note that

$$\Delta_{ijk} = \Delta_{kij} = \Delta_{jki} = -\Delta_{kji} = -\Delta_{jik} = -\Delta_{ikj},$$

and if $j = k, k = i, j = i$ then

$$\Delta_{ijk} = 0.$$

Let

$$\rho_0 = \frac{m_0}{m_3},\ \rho_1 = \frac{m_1}{m_3},\ \rho_2 = \frac{m_2}{m_3}, \tag{3.4}$$

where ρ_0, ρ_1 and ρ_2 are positive mass ratio. When we make the substitutions as described in equations (3.2), (3.3), and (3.4), equation (3.1) transforms into the following form

$$\left.\begin{aligned}
f_{01} &= \rho_2(b-a)\left(\frac{1}{\tau}-\frac{1}{\sigma}\right) + \left(\frac{1}{T}-\frac{1}{M}\right)(b+bc_1-c_2) = 0,\\
f_{02} &= \rho_1(\frac{1}{\varsigma}-\frac{1}{\sigma}) - (\frac{1}{T}-\frac{1}{G})c_1 = 0,\\
f_{03} &= \rho_1\left(\frac{1}{\varsigma}-\frac{1}{M}\right)(c_2-b-bc_1) - \rho_2(b-a)\left(\frac{1}{\tau}-\frac{1}{G}\right)c_1,\\
f_{12} &= \rho_0(b-a)\left(\frac{1}{\varsigma}-\frac{1}{\tau}\right) + \left(\frac{1}{M}-\frac{1}{G}\right)(c_2-a-ac_1=0),\\
f_{13} &= \rho_0\left(\frac{1}{\varsigma}-\frac{1}{T}\right)(c_2-b-bc_1) + \rho_2\left(\frac{1}{\sigma}-\frac{1}{G}\right)(c_2-a-ac_1) = 0,\\
f_{23} &= \rho_0(a-b)\left(\frac{1}{\tau}-\frac{1}{T}\right)c_1 - \rho_1\left(\frac{1}{\sigma}-\frac{1}{M}\right)(c_2-a-ac_1) = 0.
\end{aligned}\right\} \tag{3.5}$$

Remark 1 With the selected coordinates, it is possible to achieve every conceivable geometric configuration of four bodies in a non-collinear planar arrangement while maintaining constant values for a, b, c_1, and c_2.

To illustrate this, consider the following examples: when $c_1 = 1$, $c_2 = 0$, and $b > 0$, we will obtain a concave kite configuration, as shown in figure 3.1. If we set c_1 = -1 and b = 0, the result will be a right trapezoid configuration, as depicted in figure 3.2.

Lastly, with $c_1 = 1$, $c_2 = 0$, and $b < 0$, we will achieve a convex kite configuration, as illustrated in figure 3.3.

3.1.2 Conditions for the Existence of Central Configurations in the Four-Body Problem

Theorem 1 Examine a four-body problem with four masses m_0, m_1, m_2 and m_3 and position vectors $\mathbf{r_0} = (0,\ b)$, $\mathbf{r_1} = (1,\ 0)$, $\mathbf{r_2} = (0,\ a)$, $\mathbf{r_3} = (c_1, c_2)$ where $a, b, c_1, c_2 \in \mathbb{R}$ with a > 0, $b \neq \pm a$ and $\sigma \neq \varsigma$, $\tau \neq \sigma$, $\tau \neq \varsigma$. In order for $\mathbf{r} = (\mathbf{r_0},\ \mathbf{r_1},\ \mathbf{r_2},\ \mathbf{r_3})$ to be a CC, there exist unique mass ratios,

$$\left.\begin{aligned} \rho_0 &= \frac{(c_2 - a - ac_1)(M - G)\varsigma\tau}{(a-b)(\varsigma - \tau)MG}, \\ \rho_1 &= \frac{c_1(G - T)\sigma\varsigma}{(\sigma - \varsigma)GT}, \\ \rho_2 &= \frac{(c_2 - b - bc_1)(M - T)\sigma\tau}{(a-b)(\tau - \sigma)MT}, \end{aligned}\right\} \tag{3.6}$$

subject to the constraint,

$$\psi(a, b, c_1, c_2) = \tau(\sigma - \varsigma)M + T((\tau - \sigma)M + \sigma(\varsigma - \tau)) + G((\sigma - \varsigma)T + (\varsigma - \tau)M + \varsigma(\tau - \sigma)) = 0, \tag{3.7}$$

where $\sigma = (1+a^2)^{\frac{3}{2}}$, $\varsigma = (1+b^2)^{\frac{3}{2}}$, $\tau = (a-b)^3$, $G = (c_1^2 + (c_2 - a)^2)^{\frac{3}{2}}$, $T = (c_1^2 + (c_2 - b)^2)^{\frac{3}{2}}$, $M = (c_2^2 + (c_1 + 1)^2)^{\frac{3}{2}}$ [2].

Proof Assume $\varsigma \neq \tau \neq \sigma$, then solving $f_{12} = 0$, $f_{02} = 0$ and $f_{01} = 0$ of equations (3.5) for ρ_0, ρ_1 and ρ_2, respectively, and simplifying the corresponding expressions, we obtain equation (3.6).

Substituting the expressions of ρ_0, ρ_1 and ρ_2 into $f_{03} = 0$, $f_{13} = 0$ and $f_{23} = 0$ of equation (3.5), we get

$$c_1(c_2 - b - bc_1)\psi_1(a, b, c_1, c_2) = 0, \tag{3.8}$$

$$(c_2 - a - ac_1)(c_2 - b - bc_1)\psi_2(a, b, c_1, c_2) = 0, \tag{3.9}$$

$$c_1(c_2 - a - ac_1)\psi_3(a, b, c_1, c_2) = 0, \tag{3.10}$$

where

$$\psi_1(a, b, c_1, c_2) = \frac{\left(\frac{1}{T} - \frac{1}{G}\right)\left(\frac{1}{\varsigma} - \frac{1}{M}\right)}{\left(\frac{1}{\varsigma} - \frac{1}{\sigma}\right)} - \frac{\left(\frac{1}{T} - \frac{1}{M}\right)\left(\frac{1}{\tau} - \frac{1}{G}\right)}{\left(\frac{1}{\tau} - \frac{1}{\sigma}\right)}, \tag{3.11}$$

$$\psi_2(a,b,c_1,c_2)=\frac{\left(\frac{1}{M}-\frac{1}{G}\right)\left(\frac{1}{\varsigma}-\frac{1}{T}\right)}{\left(\frac{1}{\varsigma}-\frac{1}{\tau}\right)}-\frac{\left(\frac{1}{T}-\frac{1}{M}\right)\left(\frac{1}{\sigma}-\frac{1}{G}\right)}{\left(\frac{1}{\tau}-\frac{1}{\sigma}\right)}, \tag{3.12}$$

$$\psi_3(a,b,c_1,c_2)=\frac{\left(\frac{1}{T}-\frac{1}{G}\right)\left(\frac{1}{\sigma}-\frac{1}{M}\right)}{\left(\frac{1}{\varsigma}-\frac{1}{\sigma}\right)}-\frac{\left(\frac{1}{M}-\frac{1}{G}\right)\left(\frac{1}{\tau}-\frac{1}{T}\right)}{\left(\frac{1}{\varsigma}-\frac{1}{\tau}\right)}. \tag{3.13}$$

Equation (3.9), (3.10), (3.8) consist of $\psi_i(a,b,c_1,c_2)=0$, $i=1,2,3$ and the straight lines $c_1=0$, $c_2-b-bc_1=0$ and $c_2-a-ac_1=0$. Under the assumptions $\tau\neq\sigma$ and $\tau\neq\varsigma$, we will demonstrate that these three lines do not impose any constraint.

From assumption $\varsigma\neq\sigma$, it is easy to see that $f_{02}=0$ implies $c_1\neq 0$. Similarly, in the case of $\tau\neq\sigma$ and $\tau\neq\varsigma$, $f_{01}=0$ implies $c_2-b-bc_1\neq 0$ and $f_{12}=0$ implies $c_2-a-ac_1\neq 0$. Therefore, equation (3.9), (3.10), (3.8) reduce to the following three equations

$$\left.\begin{aligned}\psi_1(a,b,c_1,c_2)&=0,\\ \psi_2(a,b,c_1,c_2)&=0,\\ \psi_3(a,b,c_1,c_2)&=0.\end{aligned}\right\} \tag{3.14}$$

Simplifying equations (3.14), we get

$$\left.\begin{aligned}\frac{\sigma\psi(a,b,c_1,c_2)}{MGT(\sigma-\varsigma)(\sigma-\tau)}&=0,\\ \frac{\tau\psi(a,b,c_1,c_2)}{MGT(\varsigma-\tau)(\tau-\sigma)}&=0,\\ \frac{\varsigma\psi(a,b,c_1,c_2)}{MGT(\sigma-\varsigma)(\varsigma-\tau)}&=0,\end{aligned}\right\} \tag{3.15}$$

where

$$\begin{aligned}\psi(a,b,c_1,c_2)=\tau(\sigma-\varsigma)M+T((\tau-\sigma)M+\sigma(\varsigma-\tau))\\ +G((\sigma-\varsigma)T+(\varsigma-\tau)M+\varsigma(\tau-\sigma)).\end{aligned} \tag{3.16}$$

Under the above assumptions, equation (3.15) lead to

$$\psi(a,b,c_1,c_2)=0. \tag{3.17}$$

Equation (3.17) establishes a prerequisite for the presence of four-body central configurations. To ensure that these central configurations have significance, it is essential that the mass ratios ρ_0, ρ_1, and ρ_2 are all positive.

3.1.3 Constraints Arising from All Masses Being Positive

We establish the following lemmas, which are valuable in examining the positivity of mass ratios and in deriving regions for central configurations where all masses are confirmed to be positive [2].

Lemma 1 Let $I = u^{3/2}$ and $J = v^{3/2}$ with u > 0 and v > 0. Then

$$I - J = (uv)E^{+}_{IJ}, \tag{3.18}$$

where the factor $E^{+}_{IJ} > 0$ is given by

$$E^{+}_{IJ} = \frac{I^{2/3} + J^{2/3} + (IJ)^{1/3}}{I^{1/3} + J^{1/3}}. \tag{3.19}$$

Proof

$$\begin{aligned} I - J = u^{3/2} - v^{3/2} =& ((\sqrt{u})^3 - (\sqrt{v})^3), \\ =& (\sqrt{u} - \sqrt{v})(u + v + \sqrt{uv}), \\ =& (u - v)\left(\frac{u + v + \sqrt{uv}}{\sqrt{u} + \sqrt{v}}\right), \\ =& (u - v)\left(\frac{I^{2/3} + J^{2/3} + (IJ)^{1/3}}{I^{1/3} + J^{1/3}}\right). \end{aligned}$$

In the subsequent lemma, we express the non-linear factors in the formulas for ρ_0, ρ_1, and ρ_2 as combinations of linear factors involving c_1 and c_2.

This facilitates the derivation of analytical expressions for the specific regions where CC exist, and where the mass ratios are confirmed to be positive.

Lemma 2 The mass ratios ρ_0, ρ_1 and ρ_2 as defined in equation (3.6) can be expressed in the following form [2]:

$$\rho_0 = \frac{(c_2 - a - ac_1)(2ac_2 + 2c_1 + 1 - a^2)\varsigma\tau E^+_{MG}}{(a-b)(1 - a_2 + 2ab)MGE^+_{\varsigma\tau}}, \tag{3.20}$$

$$\rho_1 = \frac{c_1(a + b - 2c_2)\sigma\varsigma E^+_{GT}}{(a+b)GTE^+_{\sigma\varsigma}}, \tag{3.21}$$

$$\rho_2 = \frac{(c_2 - b - bc_1)(2bc_2 + 2c_1 + 1 - b^2)\tau\sigma E^+_{MT}}{(a-b)(b^2 - 2ab - 1)MTE^+_{\tau\sigma}}. \tag{3.22}$$

The positive factors denoted as $E^+_{(IJ)}$ are defined in equation (3.19).

Proof By applying Lemma 1 and equations (3.2), we can derive the following factorization for $M - G$ and $\varsigma - \tau$.

$$M - G = (2c_1 + 2ac_2 + 1 - a^2)E^+_{MG},$$

$$\varsigma - \tau = (1 + b^2 - (a-b)^2)E^+_{\varsigma\tau}.$$

After substituting these expressions into equation (3.6), we arrive at the expression for ρ_0 as provided. The factorizations for $G - T$, $\sigma - \varsigma$, $\tau - \sigma$ and $M - T$ are presented below,

$$G - T = (a-b)(a + b - 2c_2E^+_{GT}),$$

$$\sigma - \varsigma = (a^2 - b^2)E^+_{\sigma\varsigma},$$

$$M - T = (2c_1 + 2bc_2 + 1 - b^2)E^+_{TM},$$
$$\tau - \sigma = ((a-b)^2 - a^2 - 1)E^+_{\tau\sigma}.$$

Likewise, by substituting the factored forms of $G - T$, $\sigma - \varsigma$, $M - T$ and $\tau - \sigma$ into equation (3.6), we derive the expressions for ρ_1 and ρ_2 as provided in (3.21), (3.20).

Remark 2 Simplified equivalent expressions, which share the same signs as the mass ratios ρ_0, ρ_1, and ρ_2 are presented as follows:

$$\rho_0^* = \frac{(c_2 - a - ac_1)(2ac_2 + 2c_1 + 1 - a^2)}{(a-b)(1 - a_2 + 2ab)}, \tag{3.23}$$

$$\rho_1^* = \frac{c_1(a + b - 2c_2}{(a+b)}, \tag{3.24}$$

$$\rho_2^* = \frac{(c_2 - b - bc_1)(2bc_2 + 2c_1 + 1 - b^2)}{(a-b)(b^2 - 2ab - 1)}, \tag{3.25}$$

where ρ_0^*, ρ_1^* and ρ_2^* are also positive mass ratio which is simplified form of ρ_0, ρ_1 and ρ_2.

3.1.4 Determining Areas of Central Configurations Exhibiting Non-Negative Mass Ratios

Lemma 2 has greatly facilitated the process of identifying potential regions for CC in which all mass ratios are positive. For instance, it is evident that $\rho_1 > 0$ in the following region [2],

$$S\rho_1 = \{(a, b, c_1, c_2) | c_2 \in \mathbb{R} \wedge ((b < 2c_2 \wedge ((0 < a < 2c_2 - b \wedge c_1 < 0)$$

$$\vee (a > 2c_2 - b \wedge c_1 > 0))) \vee (b \geq 2c_2 \wedge a > 0 \wedge c_1 > 0))\}. \tag{3.26}$$

Likewise, ρ_0 and ρ_2 are non negative in the areas S_{ρ_0} and S_{ρ_2} given as.

$$S_{\rho_0} = \{(a, b, c_1, c_2) | c_2 \in \mathbb{R} \wedge ((\mathcal{A}_2 < -c_2 \wedge ((\mathcal{A}_3 \leq 0 \wedge a > 0 \wedge \mathcal{A}_1 < c_2) \vee (\mathcal{A}_3 > 0$$

$$\wedge((0 < a < \mathcal{A}_3 \wedge \mathcal{A}_1 > c_2) \vee (a > \mathcal{A}_3 \wedge \mathcal{A}_1 < c_2))))) \vee (\mathcal{A}_2 > c_2 \wedge ((\mathcal{A}_3 0 \wedge a > 0 \wedge \mathcal{A}_1 > c_2)$$

$$\vee (\mathcal{A}_3 > 0 \wedge ((0 < a < \mathcal{A}_3 \wedge \mathcal{A}_1 < c_2) \vee (a > \mathcal{A}_3 \wedge \mathcal{A}_1 > c_2))))))\}, \tag{3.27}$$

and

$$S_{\rho_2} = \{(a, b, c_1, c_2) | c_2 \in \mathbb{R} \wedge a > 0 \wedge ((\mathcal{B}_2 < -c_2 \wedge ((\mathcal{B}_3 \leq 0 \wedge ((b < \mathcal{B}_3 \wedge \mathcal{B}_1 > c_2)$$

$$\vee (\mathcal{B}_3 < b < 0 \wedge \mathcal{B}_1 < c_2) \vee (b > 0 \wedge \mathcal{B}_1 > c_2))) \vee (\mathcal{B}_3 > 0 \wedge ((b < 0 \wedge \mathcal{B}_1 > c_2) \vee (0 < b < \mathcal{B}_3$$

$$\wedge\mathcal{B}_1 < c_2)\vee(b > \mathcal{B}_3\wedge\mathcal{B}_1 > c_2))))\vee(\mathcal{B}_2 > -c_2\wedge((\mathcal{B}_3 \leq 0\wedge((b < \mathcal{B}_3\wedge\mathcal{B}_1 < c_2)\vee(\mathcal{B}_3 < b < 0$$

$$\wedge\mathcal{B}_1 > c_2)\vee(b > 0\wedge\mathcal{B}_1 < c_2)))\vee(\mathcal{B}_3 > 0\wedge((b < 0\wedge\mathcal{B}_1 < c_2)\vee(0 < b < \mathcal{B}_3\wedge\mathcal{B}_1 > c_2)\vee(b$$

$$> \mathcal{B}_3 \wedge \mathcal{B}_1 < c_2))))))\}, \tag{3.28}$$

where

$$\mathcal{A}_1 = a + ac_1, \mathcal{A}_2 = \frac{1-a^2}{2a} + \frac{c_1}{a}, \mathcal{A}_3 = b + \sqrt{b^2+1},$$

$$\mathcal{B}_1 = b + bc_1, \mathcal{B}_2 = \frac{1-b^2}{2b} + \frac{c_1}{b}, \mathcal{B}_3 = -a + \sqrt{a^2+1}.$$

The CC region in the general $4B$ problem, under the constraint $\psi(a, b, c_1, c_2) = 0$, is formed by the overlap of the regions S_{ρ_0}, S_{ρ_1} and S_{ρ_2}. While it is relatively straightforward to identify these CC regions for specific mass ratios individually, the process becomes considerably complex when determining their intersection. Moreover, finding the solutions to the geometric constraint $\psi(a, b, c_1, c_2) = 0$ is an even more challenging task and often necessitates the use of computer algebra systems.

3.1.5 Utilizing the Method to Identify Central Configurations in Convex and Concave Scenarios

In order to gain a better understanding of the problem, we will employ the methodology outlined above to identify CC in two specific instances of the general $4B$ coplanar problem, each involving four distinct masses. In these two examples, we will select particular values for a and b, which will consequently determine the positions of the masses, namely, m_0, m_1 and m_2. Subsequently, we will assess the essential condition $\psi(c_1, c_2) = 0$ to determine whether central configurations exist in these cases.

Central Configuration $a = 0.9$ and $b = -0.1$

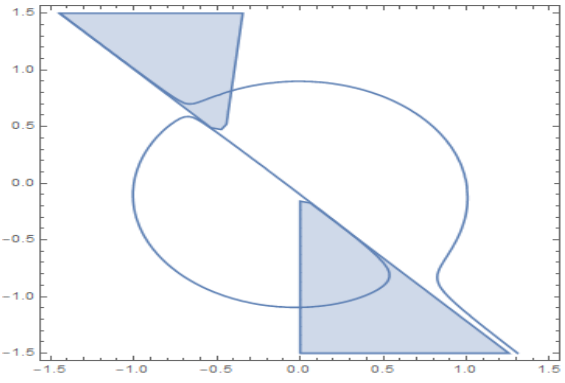

FIGURE 3.1: Central Configurations for $(a, b) = (0.9, -0.1)$

For $a = 0.9$ and $b = -0.1$ above Figure(3.1) shows a family of CC defined by parameters a and b. The shaded region represents the set of CC where all masses involved are non negative. The blue line represents a constraint, specifically $\psi(c_1, c_2) = 0$, which is associated with these CC. In [2] Shoaib et.al. have discussed the following two CC cases.

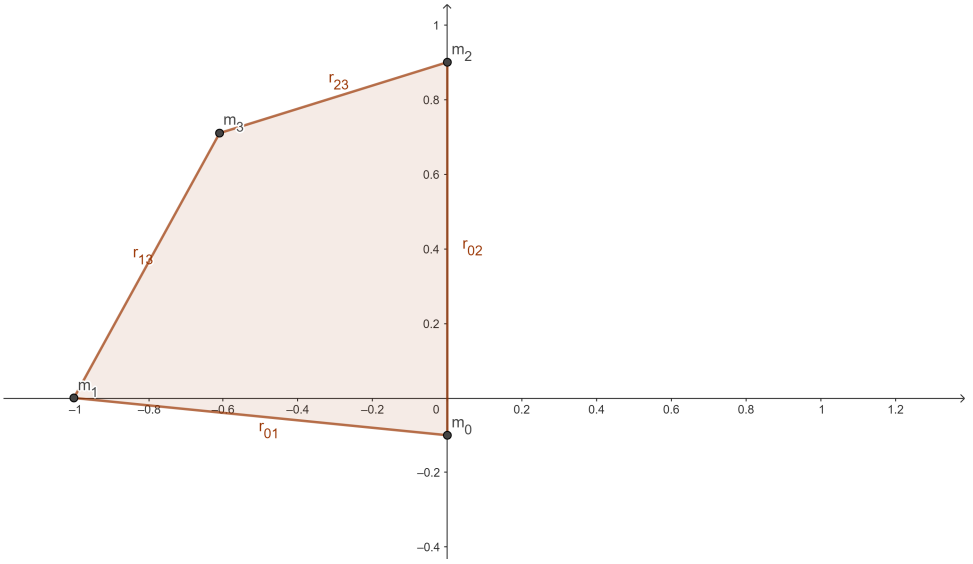

FIGURE 3.2: Specific Central Configurations for $(a, b) = (0.9, -0.1)$

1) They have chosen the values of $c_1 = -0.61$ and $c_2 = 0.71$. The associated values of mass parameters is $(\rho_0, \rho_1, \rho_2) = (47.32, 3.05, 1.17)$.

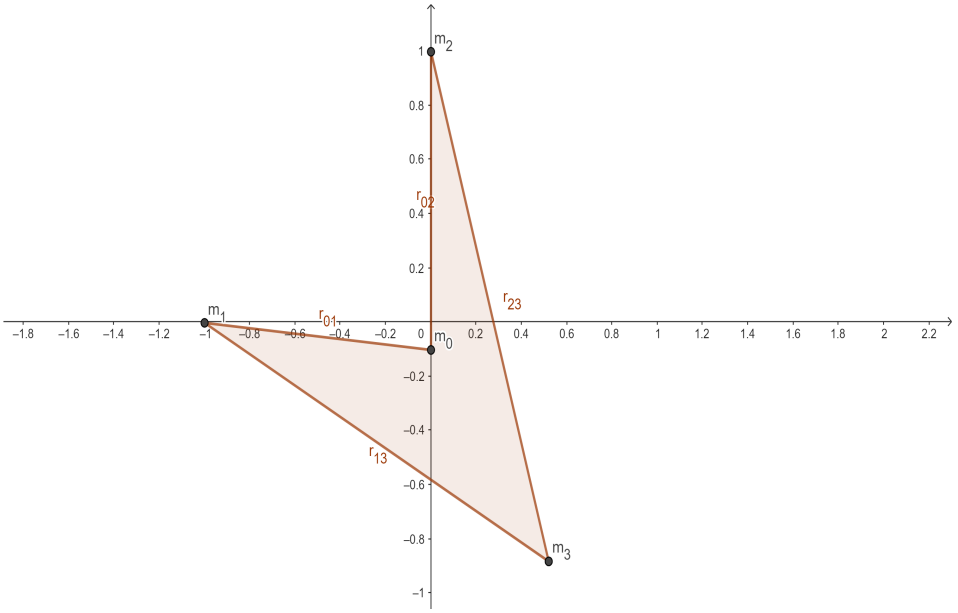

FIGURE 3.3: Specific Central Configurations for $(a, b) = (0.9, -0.1)$

2) They have chosen the values of $c_1 = 0.52$ and $c_2 = -0.88$. The associated values of mass parameters is $(\rho_0, \rho_1, \rho_2) = (4.21, 0.96, 1.27)$.

Central Configuration $a = 1.5$ and $b = 0.4$

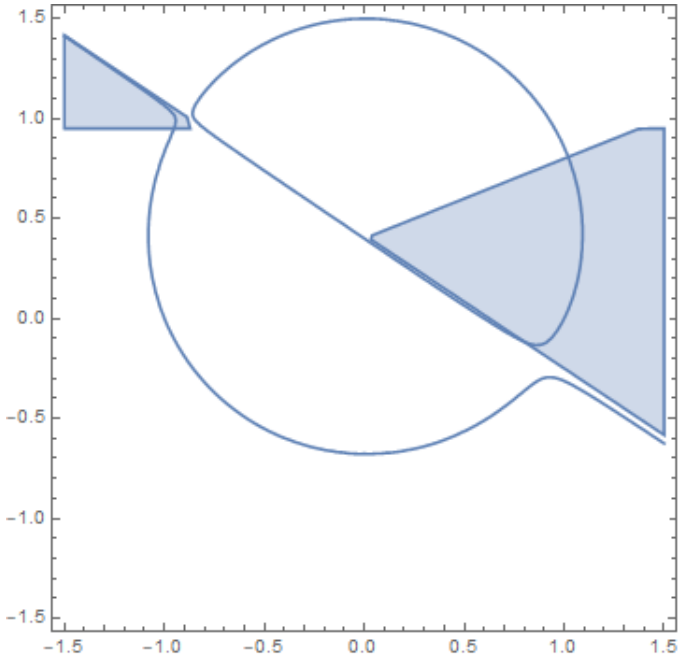

FIGURE 3.4: Central Configurations for $(a, b) = (1.5, 0.4)$

For $(a, b) = (1.5, 0.4)$ above Figure(3.4) shows a family of CC, just like in the previous figure, but with different values of a and b 1.5 and 0.4, respectively. The shaded region represents the CC where all masses are non negative. The blue line represents the constraint $\psi(c_1, c_2) = 0$, which is associated with these central configurations. In [2] Shoaib et.al. have discussed the following two CC cases.

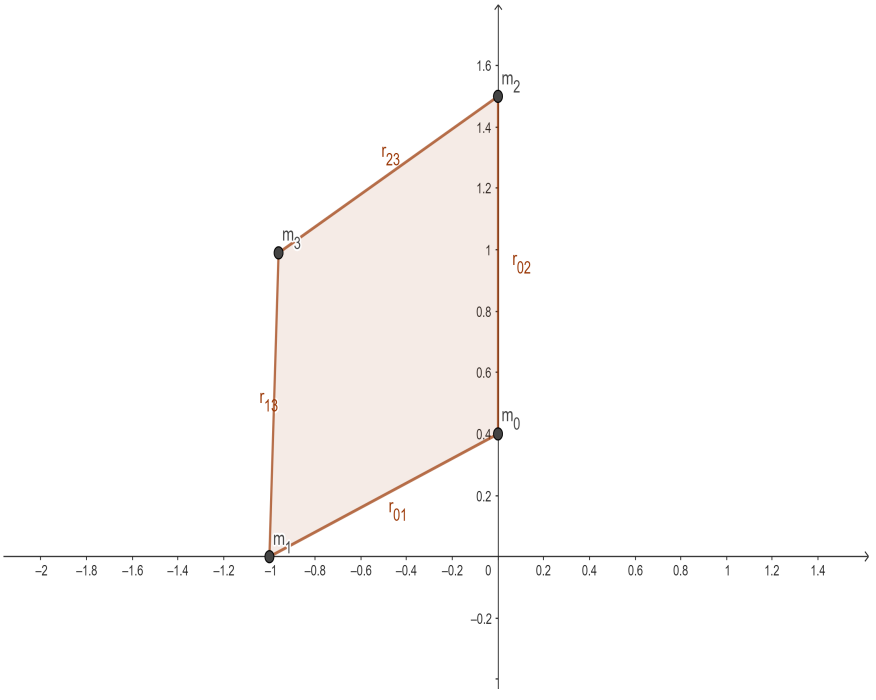

FIGURE 3.5: Specific Central Configurations for $(a, b) = (1.5, 0.4)$

1) They have chosen the values of $c_1 = -0.96$ and $c_2 = 0.99$. The associated values of mass parameters is $(\rho_0, \rho_1, \rho_2) = (3.64, 0.15, 0.48)$.

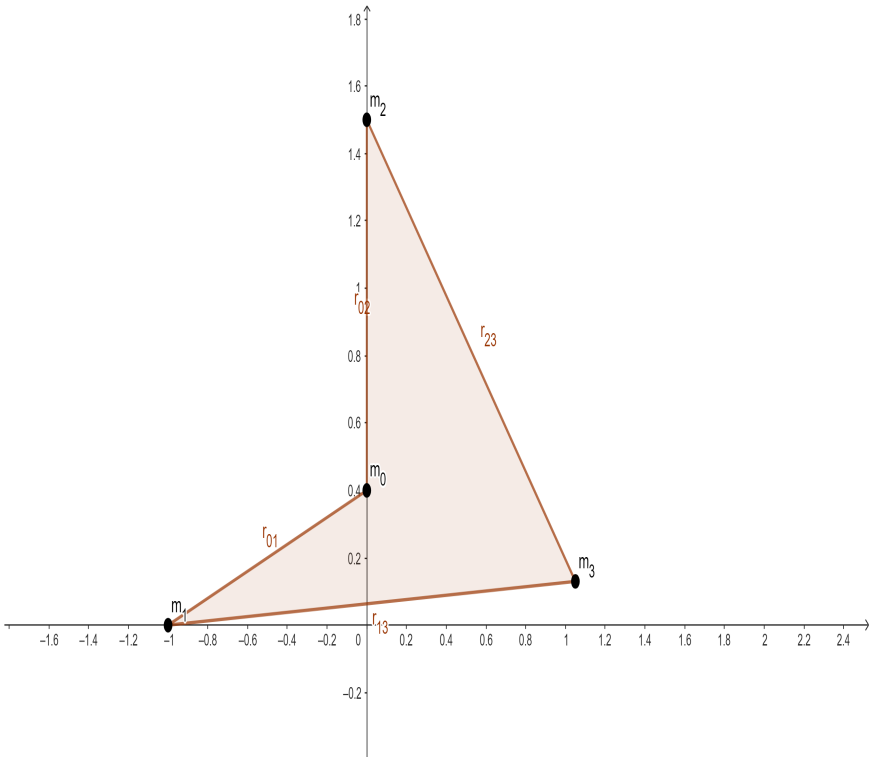

FIGURE 3.6: Specific Central Configurations for $(a, b) = (1.5, 0.4)$

2) They have chosen the values of $c_1 = 1.05$ and $c_2 = 0.13$. The associated values of mass parameters is $(\rho_0, \rho_1, \rho_2) = (4.31, 0.98, 0.72)$.

Chapter 4

Dynamic of Fifth Body in the Central Configuration of Primary Bodies

In this extended study, we explore a constrained restricted five-body scenario involving four distinct positive masses designated as m_0, m_1, m_2 and m_3. Three of these masses are positioned at the vertices of a triangle, while the fourth mass is allowed to occupy any point in the plane, creating convex or concave CC. Simultaneously, a smaller mass, denoted as m_4, moves within the same plane, influenced by the gravitational forces exerted by the four primary masses (m_0, m_1, m_2, m_3). It is crucial to emphasize that the motion of m_4 does not influence the movement of the four primary masses.

To analyze this complex system, our objectives include determining the positions of equilibrium points and evaluating their stability. Additionally, we aim to investigate the Newton basins of attraction for these equilibrium points. This involves studying how the system behaves near these points under gravitational influences, providing insights into the dynamics and stability of the entire configuration.

We will formulate the equation of motion for the fifth particle with restricted motion and mass m_4, considering an inertial frame of reference,

$$m_i \ddot{\mathbf{r}}_i = \nabla_i U_i \qquad\qquad i = 1, ..., n \tag{4.1}$$

$$m_i\ddot{\mathbf{r}}_i = -G\sum_{i=1,j=1,i\neq j}^{n}\frac{m_i m_j}{|r_i - r_j|^3}\mathbf{r}_{ij},$$

$\mathbf{r_i}$ and m_i are the position vector and mass of the i^{th} body respectively and G is the constant of gravitation,

$$\ddot{\mathbf{r_4}} = m_0\frac{r_0 - r_4}{|r_0 - r_4|^3} + m_1\frac{r_1 - r_4}{|r_1 - r_4|^3} + m_2\frac{r_2 - r_4}{|r_2 - r_4|^3} + m_3\frac{r_3 - r_4}{|r_3 - r_4|^3}. \tag{4.2}$$

We will now establish a coordinate system rotating uniformly about the center of mass, denoted by ω. In this new rotating frame, let (x, y) represent the coordinates of m_4. Our objective is to transform the equation from the original fixed inertial frame to this rotating coordinate system using the provided orthogonal system.

$$\mathbf{e_1} = e^{i\omega t}, \mathbf{e_2} = ie^{i\omega t},$$

in the context of this rotating frame, where ω denotes the angular speed and "t" represents time, the position vector of m_4 can be expressed as follows:

$$\mathbf{r_4} = x(t)\mathbf{e_1} + y(t)\mathbf{e_2}. \tag{4.3}$$

Selecting ω without any loss of generality and computing the first and second derivatives of equation (4.3) results in:

$$\begin{aligned}\dot{\mathbf{r_4}} =&[(\dot{x} - y) + i(x + \dot{y})]e^{it},\\ \ddot{\mathbf{r_4}} =&[(\ddot{x} - 2\dot{y} - x) + i(\ddot{y} + 2\dot{x} - y)]e^{it}.\end{aligned} \tag{4.4}$$

By substituting equation (4.4) into equation (4.2), we can express the equations of motion for m_4 in the rotating frame in component form as follows:

$$\ddot{x} - 2\dot{y} = x - \left[m_0\frac{x}{r_{40}^3} + m_1\frac{x+1}{r_{41}^3} + m_2\frac{x}{r_{42}^3} + m_3\frac{x - c_1}{r_{43}^3}\right],$$

$$\ddot{y} + 2\dot{x} = y - \left[m_0\frac{y - b}{r_{40}^3} + m_1\frac{y}{r_{41}^3} + m_2\frac{y - a}{r_{42}^3} + m_3\frac{y - c_2}{r_{43}^3}\right], \tag{4.5}$$

where mutual distances are defined as follows:

$$\begin{aligned} r_{40} =& \sqrt{x^2 + (y-b)^2}, \\ r_{41} =& \sqrt{(x+1)^2 + y^2}, \\ r_{42} =& \sqrt{x^2 + (y-a)^2}, \\ r_{43} =& \sqrt{(x-c_1)^2 + (y-c_2)^2}. \end{aligned}$$

The equation of motion for m_4 within the plane of primaries can alternatively be expressed as:

$$\Omega_x = \frac{\partial \Omega}{\partial x} = \ddot{x} - 2\dot{y}, \tag{4.6}$$

$$\Omega_y = \frac{\partial \Omega}{\partial y} = \ddot{y} + 2\dot{x}, \tag{4.7}$$

where the effective potential $\Omega(x, y)$ is:

$$\begin{aligned} \Omega(x,y) = \frac{x^2+y^2}{2} + \left[\frac{m_0}{\sqrt{x^2+(y-b)^2}} + \frac{m_1}{\sqrt{(x+1)^2+y^2}} \right] \\ + \left[\frac{m_2}{\sqrt{x^2+(y-a)^2}} + \frac{m_3}{\sqrt{(x-c_1)^2+(y-c_2)^2}} \right]. \end{aligned} \tag{4.8}$$

By comparing equations (4.5), and (4.6), (4.7) we can write equation of motion for secondary body as,

$$\Omega_x(x,y) = x - \left[m_0 \frac{x}{r_{40}^3} + m_1 \frac{x+1}{r_{41}^3} + m_2 \frac{x}{r_{42}^3} + m_3 \frac{x-c_1}{r_{43}^3} \right], \tag{4.9}$$

$$\Omega_y(x,y) = y - \left[m_0 \frac{y-b}{r_{40}^3} + m_1 \frac{y}{r_{41}^3} + m_2 \frac{y-a}{r_{42}^3} + m_3 \frac{y-c_2}{r_{43}^3} \right]. \tag{4.10}$$

The Jacobian constant is defined as follows:

$$C + \Omega = \frac{1}{2}(\dot{x^2} + \dot{y^2}) = v^2. \tag{4.11}$$

Given a specific value of the Jacobi constant, v^2 is solely dependent on the position in the rotating frame. As v^2 cannot take on negative values, it implies that,

$$C + \Omega \geq 0. \tag{4.12}$$

The borders that separate where motion is allowed from where it is not are identified by making v^2 equal to zero,

$$C + \Omega = 0. \tag{4.13}$$

4.0.1 Hill Sphere and the Region of Motion for Secondary Mass

The permitted region for motion of secondary mass is also called the hill region. Here we will discuss region of motion for different values of the Jacobian constant C for 4 different cases.

The zero-velocity curves which represent region of motion for secondary mass in Case 1 where $a = 0.9$, $b = -0.1$, $c_1 = -0.61$, $c_2 = 0.71$, $m_0 = 47.3288$, $m_1 = 3.05273$, $m_2 = 1.17191$ and $m_3 = 1$ are depicted in Figure (4.1) for three sets of mass parameters: $\rho_0 = 47.3288$, $\rho_1 = 3.05273$ and $\rho_2 = 1.17191$.

Hill spheres (circular regions) around the primary masses, are illustrated in Figure (4.1). Equation (4.10) implies that $C + \Omega$ must be greater than or equal to 0. Consequently, setting $\Omega = -C$ establishes a boundary distinguishing permitted and prohibited motions. The feasible region of motion for the infinitesimal mass m_4 in Case I, with $\rho_0 = 47.3288$, $\rho_1 = 3.05273$ and $\rho_2 = 1.17191$ is shown in Figure (4.2) for various Jacobian constant values (C).

Shaded areas denote permitted motion regions for m_4. Numerical analysis verifies that these permitted regions are interconnected when $C \geq$ -67. As C decreases, the connected permitted regions begin to disconnect, reaching complete disconnection at $C = -76.6$. Notably, the disconnection occurs in five stages, trapping m_4 entirely within the shaded region when $C \leq$ -76.6.

This disconnection pattern persists across all combinations of ρ_0, ρ_1 and ρ_2, although the number of stages may vary.

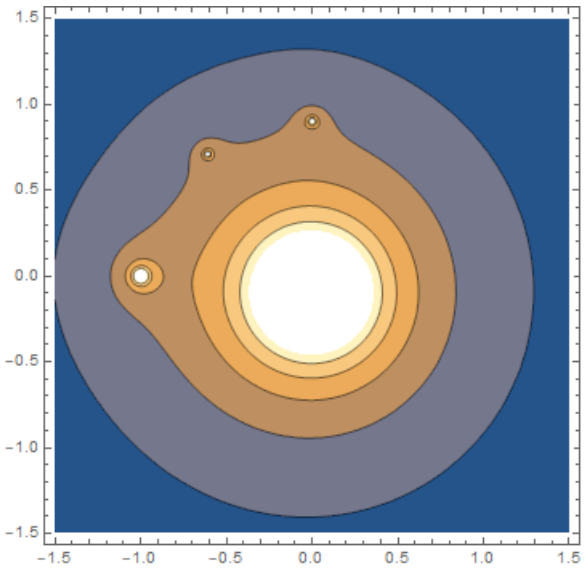

FIGURE 4.1: Case 1: Zero velocity curve for $\rho_0 = 47.3288$, $\rho_1 = 3.05273$ and ρ_2=1.17191.

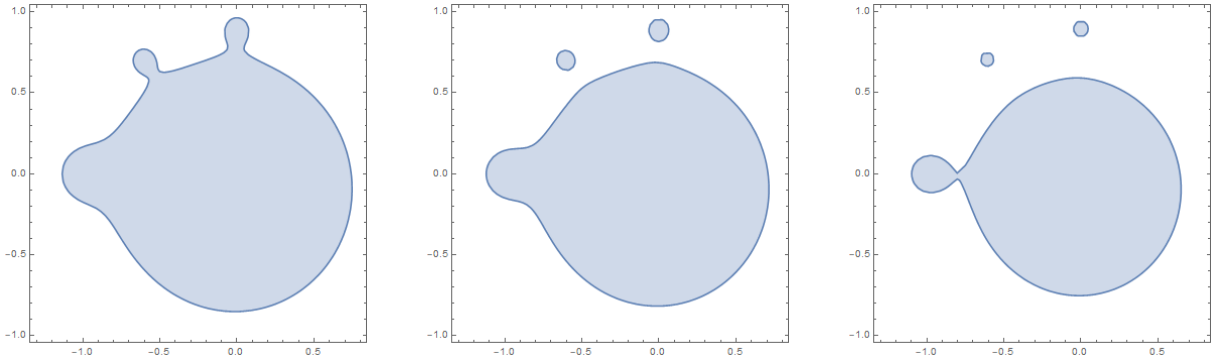

(a) (b) (c)

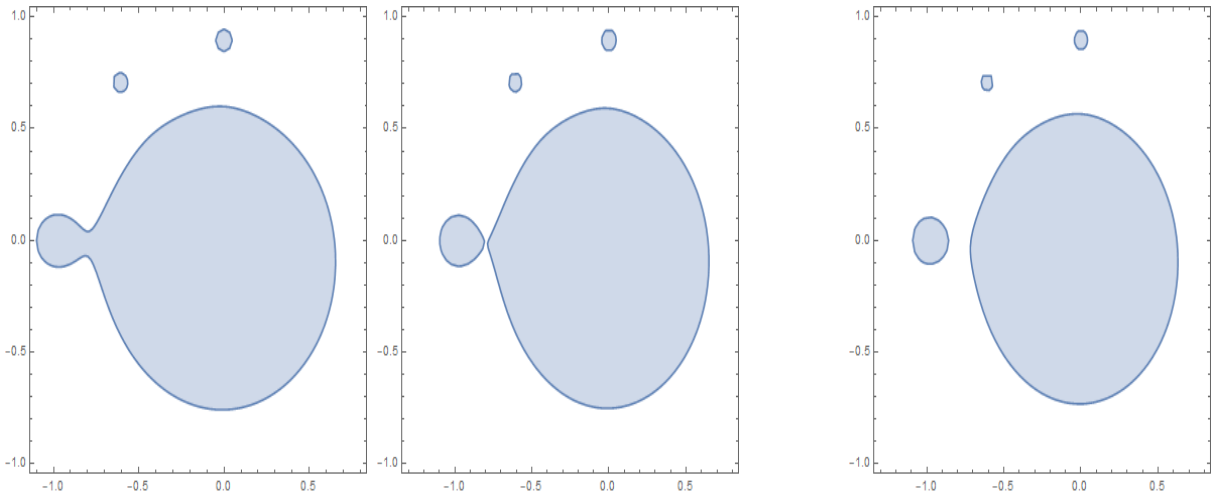

(d) (e) (f)

FIGURE 4.2: Case 1: Areas of motion for the infinitesimal mass m_4. $\rho_0 = 47.3288$, $\rho_1 = 3.05273$ and $\rho_2 = 1.17191$. (a) $C = -67$ (b) $C = -68$ (c) $C = -75$ (d) $C = -76$ (e) $C = -76.5$ (f) $C = -76.6$.

The zero-velocity curves in Case 2 where $a = 0.9$, $b = -0.1$, $c_1 = 0.52$, $c_2 = -0.88$, $m_0 = 4.21137$, $m_1 = 0.956716$, $m_2 = 1.27145$ and $m_3 = 1$ are depicted in Figure (4.3) for three sets of mass parameters: $\rho_0 = 4.21137$, $\rho_1 = 0.956716$ and $\rho_2 = 1.27145$. Hill spheres, (circular regions) around the primary masses, are illustrated in figure (4.3).

The feasible region of motion for the infinitesimal mass m_4 in Case 2, with $\rho_0 = 4.21137$, $\rho_1 = 0.956716$ and ρ_2=1.27145 is shown in Figure (4.4) for various Jacobian constant values (C). Shaded areas denote permitted motion regions for m_4. Numerical analysis verifies that these permitted regions are interconnected when $C \geq$ -10. As C decreases, the connected permitted regions begin to disconnect, reaching complete disconnection at $C = -12.2$. Notably, the disconnection occurs in five stages, trapping m_4 entirely within the shaded region when $C \leq$ -12.2.

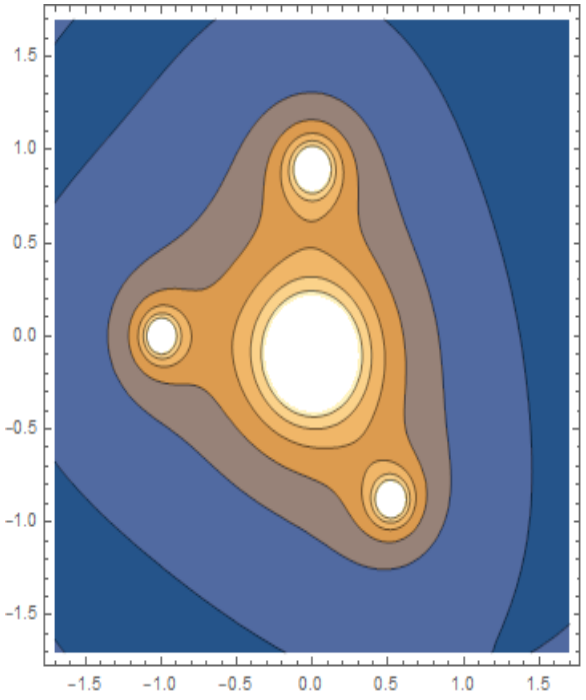

FIGURE 4.3: Case 2: Zero velocity curve for $\rho_0 = 4.21137$, $\rho_1 = 0.956716$ and ρ_2=1.27145.

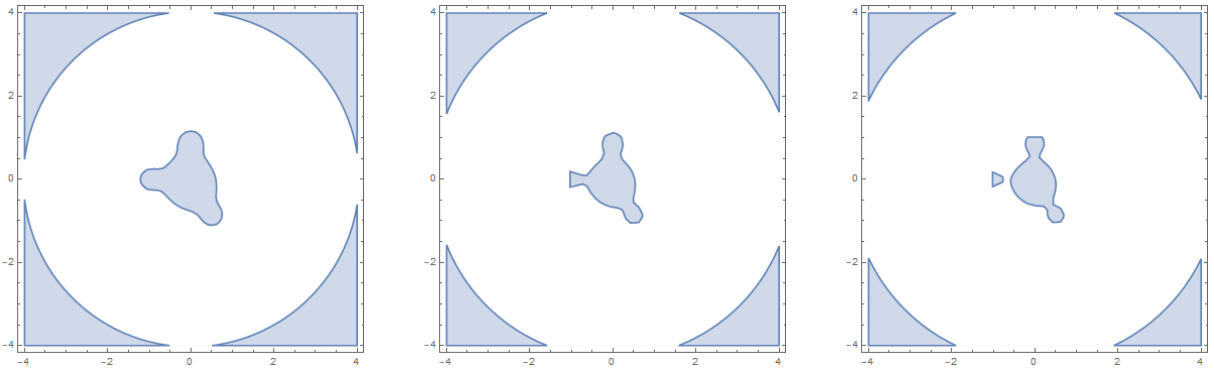

(a) (b) (c)

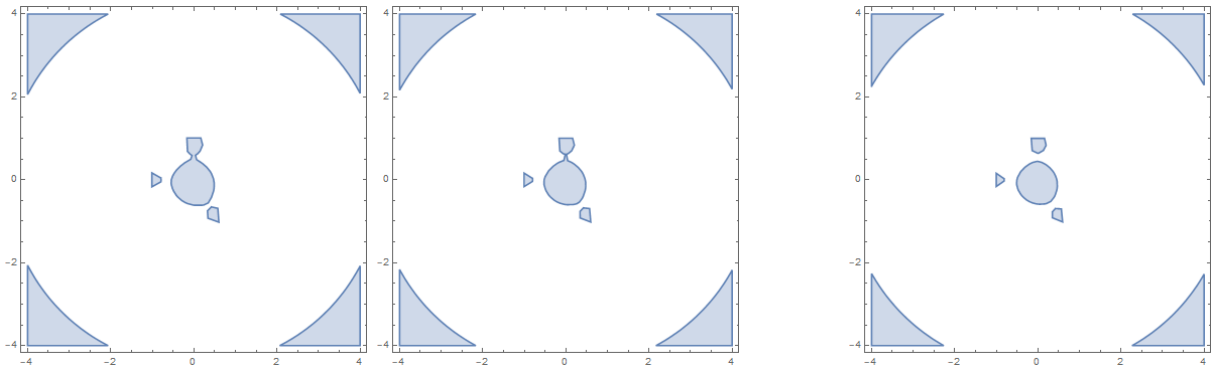

(d) (e) (f)

FIGURE 4.4: Case 2: Areas of motion for the infinitesimal mass m_4. $\rho_0 = 4.21137$, $\rho_1 = 0.956716$ and ρ_2=1.27145. (a) $C = -10$ (b) $C = -11$ (c) $C = -11.5$(d) $C = -11.8$ (e) $C = -12$ (f) $C = -12.2$.

The zero-velocity curves in Case 3 where $a = 1.5$, $b = 0.4$, c_1 = -0.96, $c_2 = 0.99999$, m_0= 3.63932, m_1=0.151366, m_2= 0.475099 and m_3= 1 are depicted in Figure (4.5) for three sets of mass parameters: $\rho_0 = 3.63932$, $\rho_1 = 0.151366$ and ρ_2=0.475099. Hill spheres, circular regions around the primary masses, are illustrated in figure (4.5).

The feasible region of motion for the infinitesimal mass m_4 in Case 3, with $\rho_0 = 3.63932$, $\rho_1 = 0.151366$ and ρ_2=0.475099 is shown in Figure (4.6) for various Jacobian constant values (C). Shaded areas denote permitted motion regions for m_4. Numerical analysis verifies that these permitted regions are interconnected when $C \geq$ -6. As C decreases, the connected permitted regions begin to disconnect, reaching complete disconnection at $C = -8.67$. Notably, the disconnection occurs in five stages, trapping m_4 entirely within the shaded region when $C \leq$ -8.67.

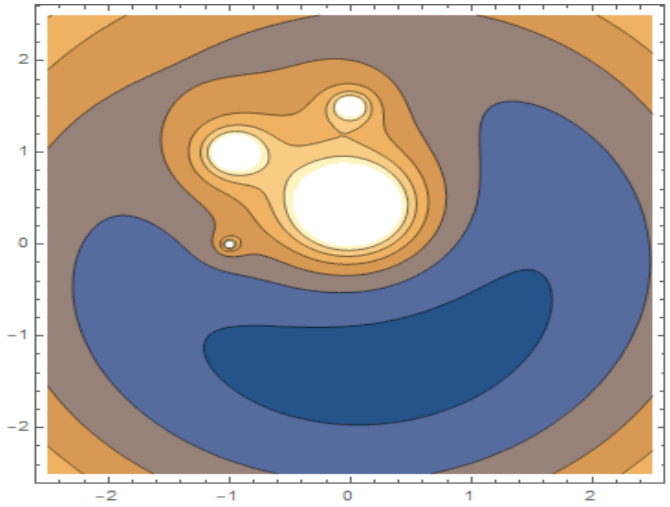

FIGURE 4.5: Case 3: Zero velocity curve for $\rho_0 = 3.63932$, $\rho_1 = 0.151366$ and ρ_2=0.475099.

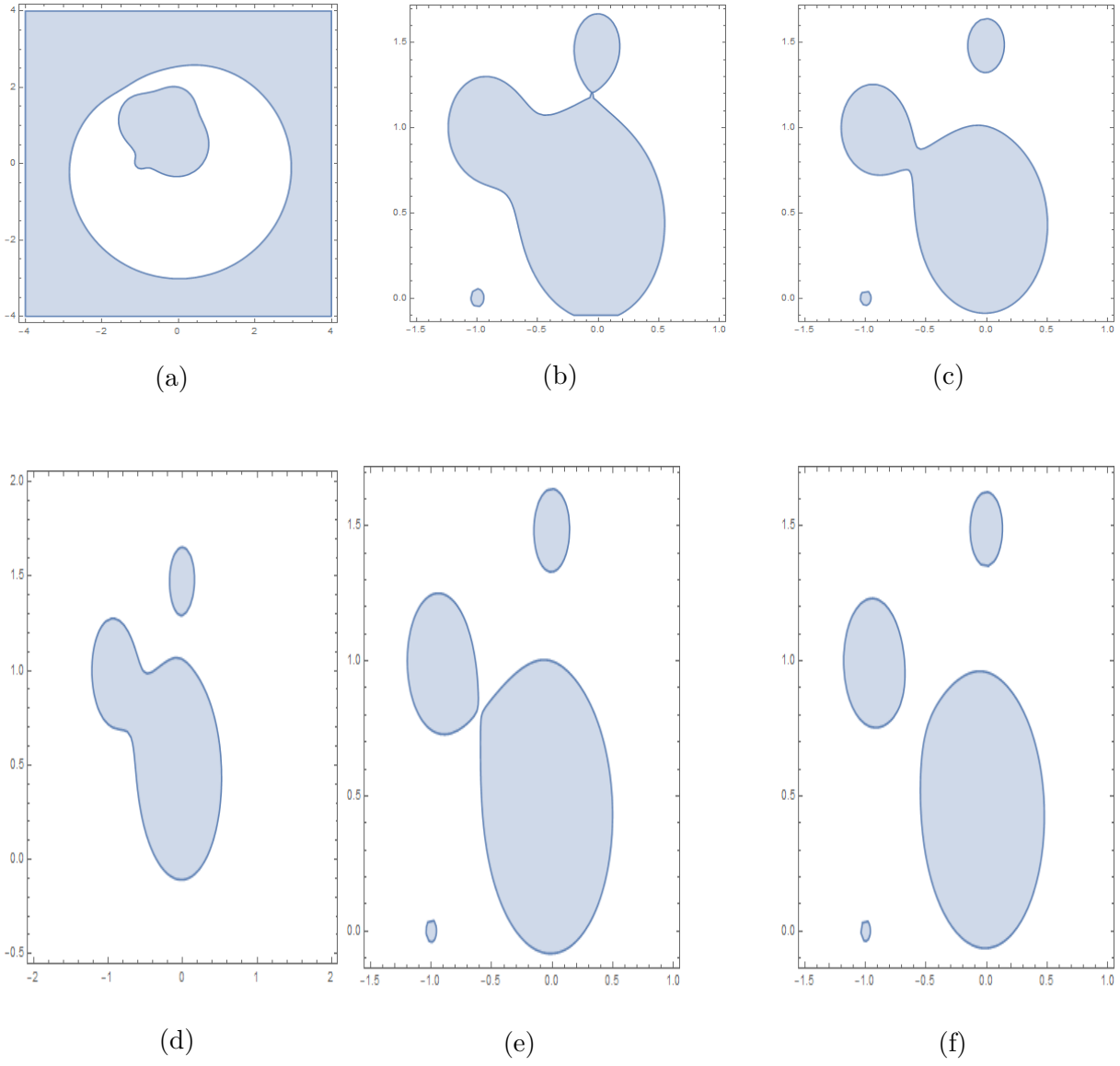

FIGURE 4.6: Case 3: Areas of motion for the infinitesimal mass m_4. $\rho_0 = 3.63932$, $\rho_1 = 0.151366$ and ρ_2=0.475099. (a) $C = -6$ (b) $C = -8$ (c) $C = -8.6$ (d) $C = -8.6$ (e) $C = -8.6$ (f) $C = -9$.

The zero-velocity curves in Case 4 where $a = 1.5$, $b = 0.4$, $c_1 = 1.05$, $c_2 = 0.13$, m_0= 4.31185, m_1=0.98422, m_2= 0.723114 and m_3= 1 are depicted in Figure (4.7) for three sets of mass parameters: $\rho_0 = 4.31185$, $\rho_1 = 0.98422$ and ρ_2=0.723114. Hill spheres, circular regions around the primary masses, are illustrated in Figure (4.7).

The feasible region of motion for the infinitesimal mass m_4 in Case 4, with $\rho_0 = 4.31185$, $\rho_1 = 0.98422$ and ρ_2=0.723114 is shown in Figure (4.8) for various Jacobian constant values (C). Shaded areas denote permitted motion regions for m_4. Numerical analysis verifies that these permitted regions are interconnected when $C \geq$ -9. As C decreases, the connected permitted regions begin to disconnect, reaching complete disconnection at $C = -10.2$. Notably, the disconnection occurs in five stages, trapping m_4 entirely within the shaded region when $C \leq$ -10.2.

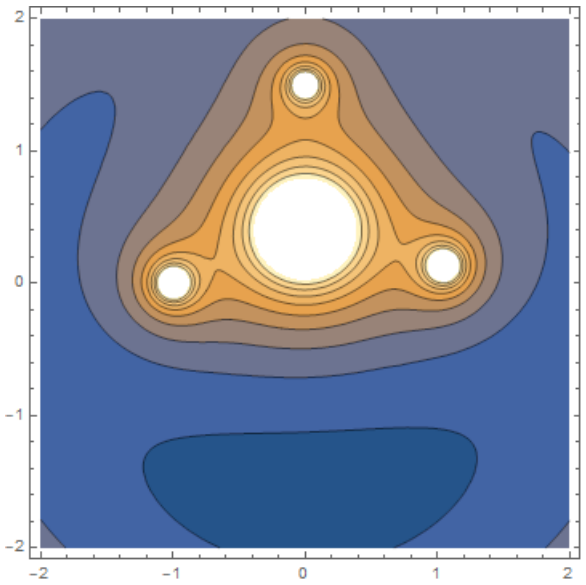

FIGURE 4.7: Case 4: Zero velocity curve for $\rho_0 = 4.31185$, $\rho_1 = 0.98422$ and ρ_2=0.723114.

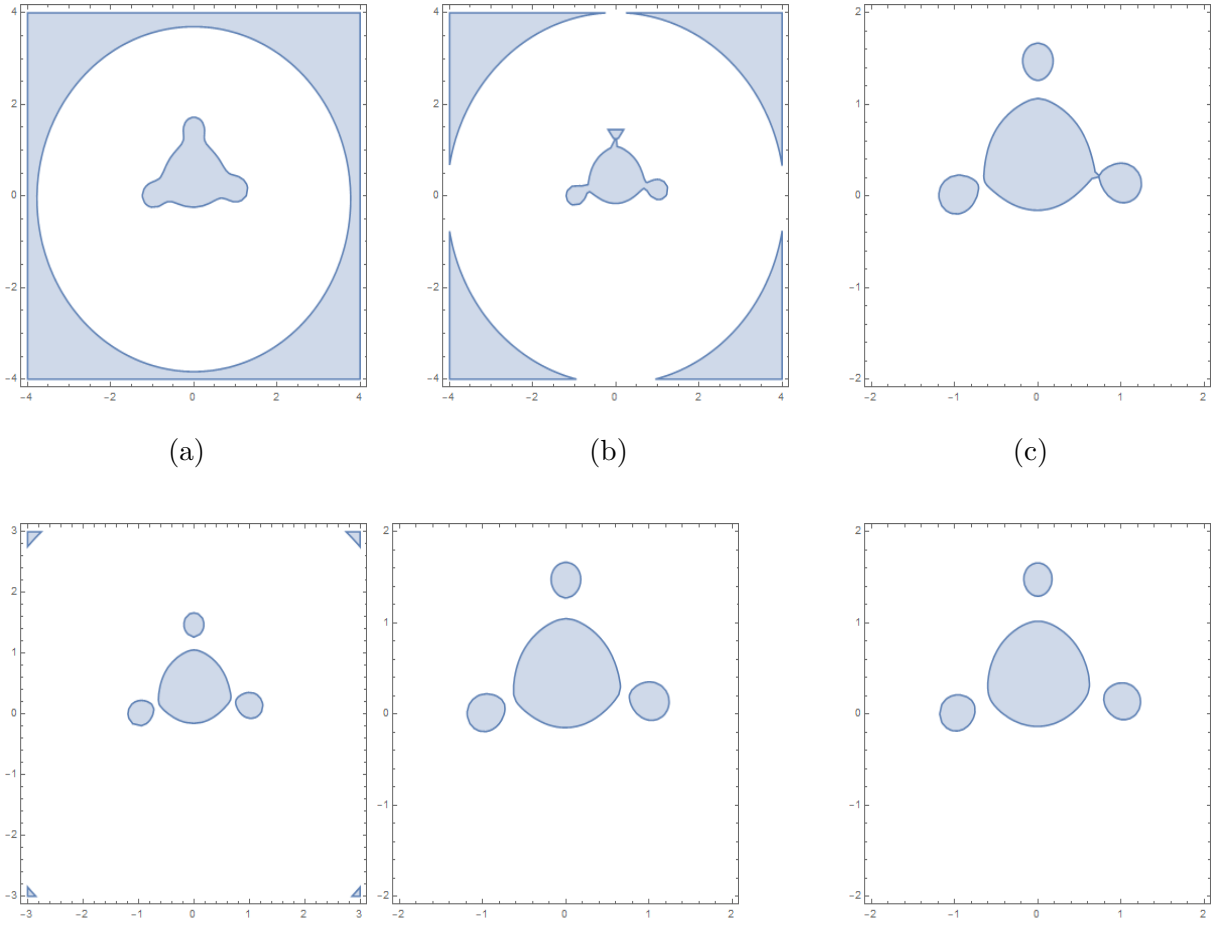

(a) (b) (c)

(d) (e) (f)

FIGURE 4.8: Case 4: Areas of motion for the infinitesimal mass m_4. ρ_0 =4.31185, ρ_1 = 0.98422 and ρ_2=0.723114. (a) $C = -9$ (b) $C = -10$ (c) $C = -10.1$ (d) $C = -10.15$ (e) $C = -10.2$ (f) $C = -10.4$.

4.0.2 Equilibrium Solutions

The solutions for equation (4.9) do not exist in a closed analytical form. However, utilizing both equations allows us to ascertain the positions of equilibrium points. These points represent locations in space where the infinitesimal mass m_4 experiences zero velocity and acceleration, meaning m_4 remains permanently at rest relative to the primaries m_0, m_1, m_2 and m_3. When situated at an equilibrium point, also referred to as Lagrange point, a body will seemingly remain fixed in that position. Discovering these solutions is necessary upon satisfying the necessary condition of having all rates equal to zero,

$$\dot{x} = \dot{y} = \ddot{x} = \ddot{y} = 0,$$

the equation (4.5) become,

$$x - \left[m_0 \frac{x}{r_{40}^3} + m_1 \frac{x+1}{r_{41}^3} + m_2 \frac{x}{r_{42}^3} + m_3 \frac{x - c_1}{r_{43}^3} \right] = 0, \tag{4.14}$$

$$y - \left[m_0 \frac{y-b}{r_{40}^3} + m_1 \frac{y}{r_{41}^3} + m_2 \frac{y-a}{r_{42}^3} + m_3 \frac{y - c_2}{r_{43}^3} \right] = 0. \tag{4.15}$$

Equations (4.13)and (4.14) exhibit significant non-linearity as they are coupled algebraic equations. In order to determine the zeros, equilibrium points, or Lagrange points, it is necessary to employ numerical methods to find equilibrium points. The categorization of equilibrium points for the Restricted Five-Body Problem ($RT5BP$) can be achieved through these numerical or graphical approaches.

The locations of equilibrium points are determined by the intersections of the non-linear equations $\Omega_x = 0$ and $\Omega_y = 0$. The positions where $\Omega_x = 0$ are marked in blue, while those where $\Omega_y = 0$ are marked in orange. The black dots indicate the positions of the primary masses, and the equilibrium points are represented by red dots in figure 4.9 to 4.13.

4.0.3 Case 1: Five Equilibrium Points and its Contour-Plot

In case 1 (discussed in Chapter 2) the values of $a = 0.9$, $b = -0.1$, $c_1 = -0.61$ and $c_2 = 0.71$ and the values of corresponding masses are $m_0 = 47.3288$, $m_1 = 3.05273$, $m_2 = 1.17191$, and $m_3 = 1$. Using these values in equations (4.15 and 4.16) and solving

numerically for (x, y) we get five roots which are given as follows: L_1=(-0.5313, 0.6081), L_2=(-0.7944, -0.01641), L_3=(-0.002206, 0.7642), L_4=(2.68, 2.536), L_5(-3.422, -1.679). The positions of these Lagrange points can be seen in the figure (4.9). The contour plot for these values reveals that L_2 aligns collinearly along the $x - axis$, whereas L_3, aligns collinearly along the $y - axis$ where L_1, L_4, and L_5 are non-collinear (figures 4.9 and 4.10).

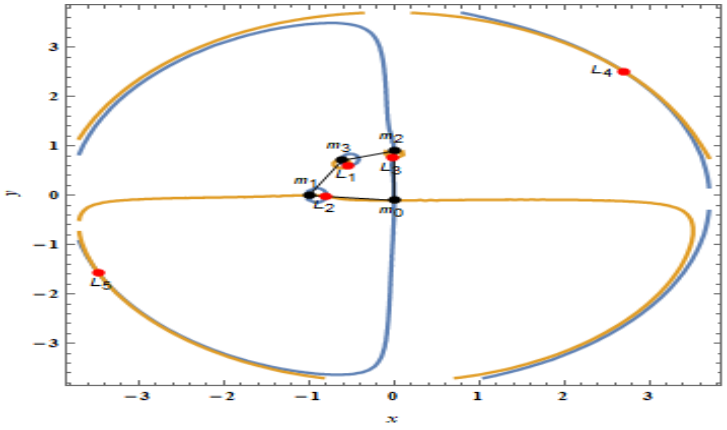

FIGURE 4.9: Case 1: Five equilibrium points black dots $a = 0.9$, $b = -0.1$, c_1=-0.61 and c_2=0.71 are primary bodies where Red dots represent the equilibrium points($L_i, i = 1, ..., 5$). Blue colour represent the region where Ω_x=0 and orange colour represent the region where Ω_y=0.

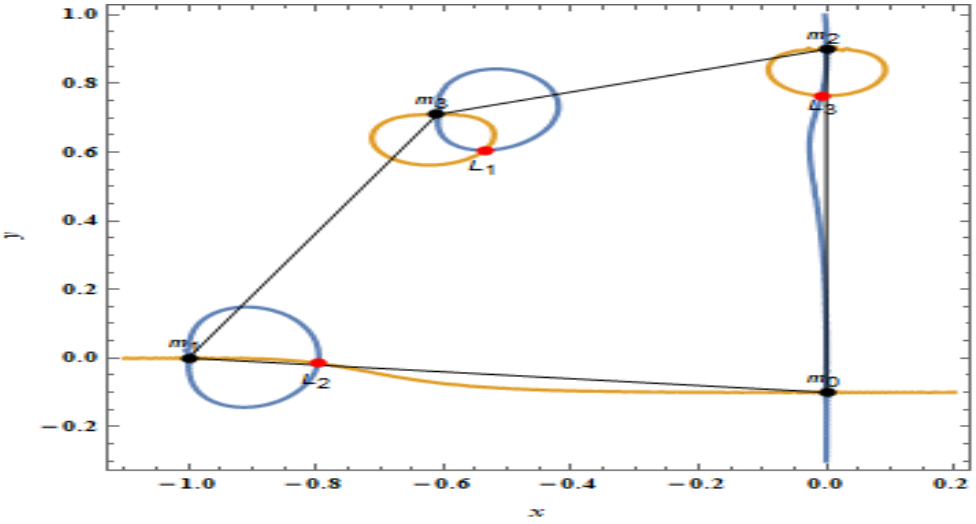

FIGURE 4.10: Figure (4.10)zoomed portion of the figure (4.9)in which L_1, L_2, L_3, L_4, and L_5 are more visible.

4.0.4 Case 2: Nine Equilibrium Points and its Contour-Plot

In case 2 (examined in Chapter 2), the equivalent masses are $m_0 = 4.21$, $m_1 = 0.96$, $m_2 = 1.27$, and $m_3 = 1$, with the values of $a = 0.9$, $b = -0.1$, $c_1 = 0.52$, and $c_2 = -0.88$. These values are used in equations (4.15 and 4.16), and numerical solutions for (x, y) are

obtained. The nine roots are as follows: L_1=(-1.348, 1.473), L_2=(-2.096, 0.03881), L_3=(-0.2338, 2.006), L_4=(-1.035, -1.647), L_5=(1.773, 0.5767), L_6=(0.961, -1.875), L_7=(0.3455, -0.6233), L_8=(-0.6786, -0.01292), L_9=(-0.01654, 0.5457), The diagram shows the locations of these Lagrange points. L_8 align collinearly along the x-axis, whereas L_9, align collinearly along the y-axis where L_1,L_2, L_3, L_4, L_5, L_6 and L_7 are non collinear, according to the contour plot for these values (figures 4.11).

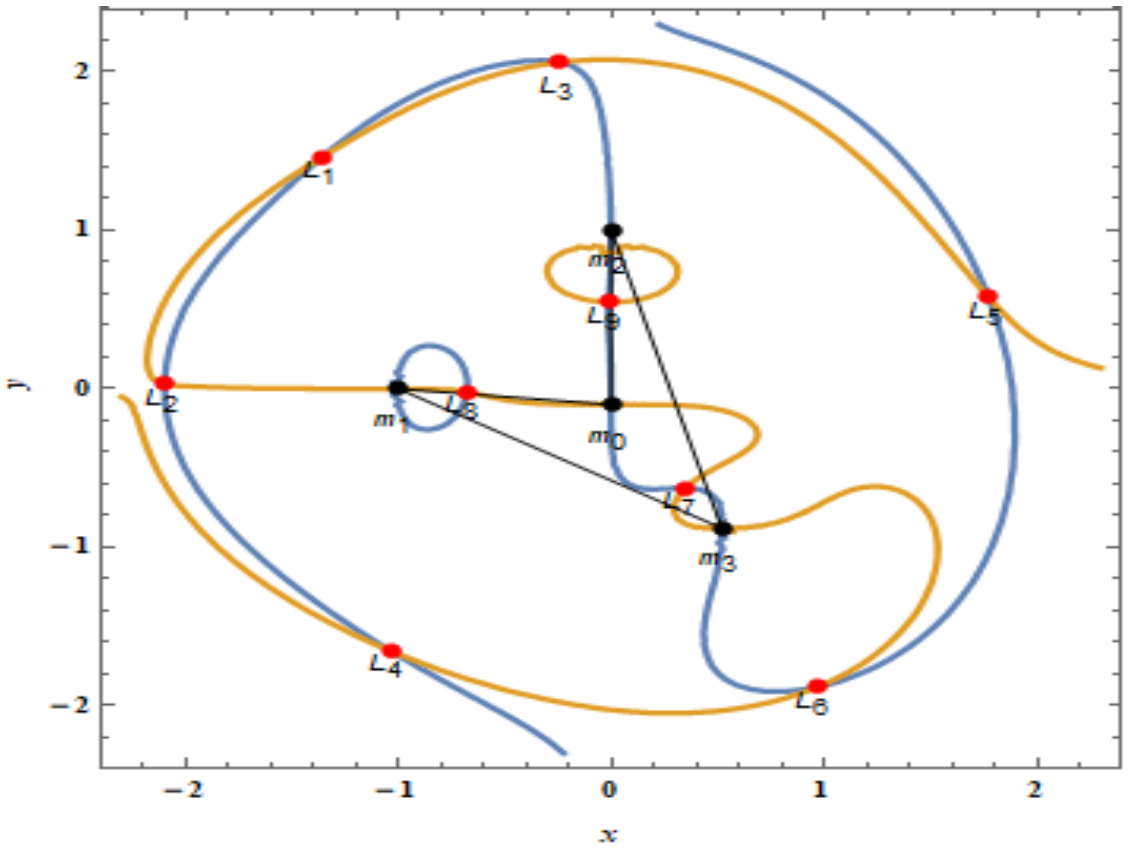

FIGURE 4.11: Case 2: Nine equilibrium points Black dots $a = 0.9$, $b = -0.1$, c_1=-0.52 and c_2=0.88 are primary bodies where Red dots represent the equilibrium points $(L_i, i = 1, ..., 9)$. Blue colour represent the region where Ω_x=0 and Orange colour represent the region where Ω_y=0.

4.0.5 Case 3: Five Equilibrium Points and its Contour-Plot

For case 2 the values of perimeter are $a = 1.5$, $b = 0.4$, $c_1 = -0.96$, and $c_2 = 0.9999$ (examined in Chapter 2), and the corresponding mass values are $m_0 = 3.64$, $m_1 = 0.15$, $m_2 = 0.48$, and $m_3 = 1$. By applying these values to equations (4.12), we may solve for (x, y) numerically and obtain five roots, which are as follows: L_1=(0.26, -1.3), L_2=(-0.85, 0.12), L_3=(-1.31, 1.87), L_4=(-0.601, 0.8147), L_5=(-0.05, 1.19). The figure shows where these Lagrange points are located. As can be seen in figures 4.12, the contour plot for these values shows that L_1,L_2, L_3, L_4 and L_5 all are non collinear.

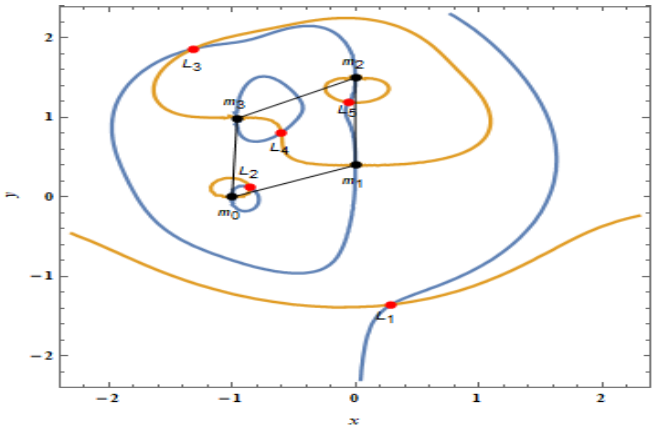

FIGURE 4.12: Case 3: Five equilibrium points Black dots $a = 1.5$, a=1.5, $b = 0.4$, c_1=-0.96 and c_2=0.99999 are primary bodies where Red dots represent the equilibrium points (L_i, $i = 1, ..., 5$). Blue colour represent the region where Ω_x=0 and Orange colour represent the region where Ω_y=0.

4.0.6 Case 4: Five Equilibrium Points and its Contour-Plot

The comparable mass values in case 4 (examined in Chapter 2) are $m_0 = 4.31$, $m_1 = 0.98$, $m_2 = 0.72$, and $m_3 = 1$. The values of $a = 1.4$, $b = 0.4$, $c_1 = 1.05$, and $c_2 = 0.13$. We obtain five roots, which are as follows, by using these values in equations (4.1) and numerically solving for (x, y), L_1(0.01602, 2.376), L_2(-0.004887, 1.183), L_3(0.7131, 0.2378), L_4(-0.681, 0.1432), L_5(0.05785, -1.595). The diagram for these values reveals that L_1 and L_2 are collinear with y-axis while L_3, L_4 and L_5 all are non collinear (figure 4.13).

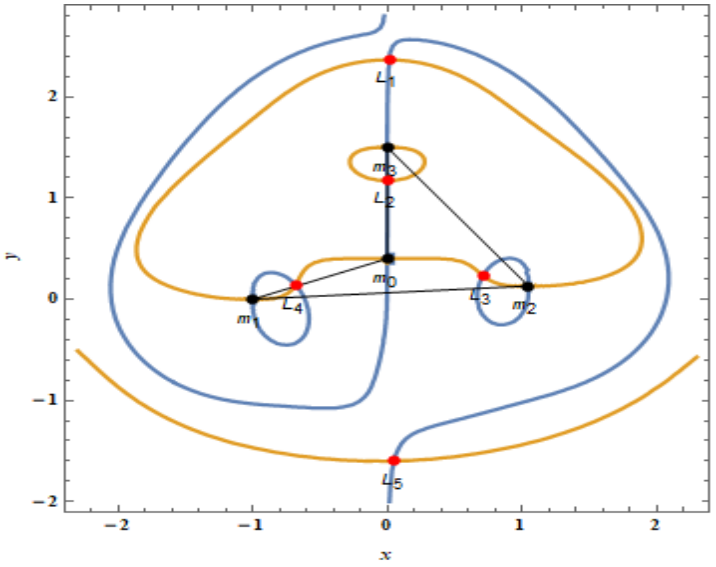

FIGURE 4.13: Case 4: Five equilibrium points Black dots $a = 1.5$, $b = 0.4$, c_1=1.o5 and c_2=0.13 are primary bodies where Red dots represent the equilibrium points ($L_i, i = 1, ..., 5$). Blue colour represent the region where Ω_x=0 and Orange colour represent the region where Ω_y=0.

4.1 Stability Analysis of Lagrange Points

To analyze the stability of the equilibrium points determined in the preceding section, we will employ the conventional linearization method by linearizing the equation of motion for the infinitesimal mass. Let the coordinates of an equilibrium point in the Restricted Five-Body Problem ($R5BP$) be represented by (x, y).
Now, consider a small displacement (X, Y) from this point, resulting in the new positions $x+X$ and $y+Y$ for the infinitesimal mass.

By applying Taylor series expansion to equations (4.6) and (4.7), we derive a new set of second-order linear differential equations.

$$\left.\begin{aligned} \ddot{X} - 2\dot{Y} &= X\Omega_{xx} + Y\Omega_{xy}, \\ \ddot{Y} + 2\dot{X} &= X\Omega_{xy} + Y\Omega_{yy}. \end{aligned}\right\} \tag{4.16}$$

The matrix representation of the linearized equations is as follows:

$$\dot{\mathbf{X}} = \mathbf{A}\mathbf{X}, \tag{4.17}$$

$$\mathbf{X}= \begin{pmatrix} \dot{x} \\ \dot{y} \\ \ddot{x} \\ \ddot{y} \end{pmatrix}, \ \mathbf{A}= \begin{bmatrix} 0 & 0 & 1 & 0 \\ 0 & 0 & 0 & 1 \\ \Omega_{xx} & \Omega_{xy} & 0 & 2 \\ \Omega_{xy} & \Omega_{yy} & -2 & 0 \end{bmatrix}.$$

By using above equation we will check stability of Lagrange points one by one.

Case 1

By taking $a = 0.9$, $b = -0.1$, c_1 = -0.61, $c_2 = 0.71$ and Lagrange points L_1=(-0.5313, 0.6081), L_2=(-0.7944, -0.01641), L_3=(-0.002206, 0.7642), L_4=(2.68, 2.536), L_5(-3.422, -1.679).
Taking these values and finding the characteristic equation for eigenvalue of matrix A using equation (4.9) the following table show the stability of $L_1 - L_5$ as follows.

Lagrange Points	Eigenvalues	Stability
L_1	$\pm 32.9294, \pm 22.9397i$	Unstable
L_2	$\pm 30.0539, \pm 21.179i$	Unstable
L_3	$\pm 32.9629, \pm 23.152i$	Unstable
L_4	$\pm 0.962003i, \pm 0.302258i$	Unstable
L_5	$\mp 0.269501, \pm 1.01691i$	Unstable

TABLE 4.1: Stability Analysis Case 1: $a = 0.9$, $b = -0.1$, c_1 = -0.61, $c_2 = 0.71$.

Case 2

By taking $a = 0.9$, $b = -0.1$, $c_1 = 0.52$, c_2 = -0.88 and Lagrange points are L_1=(-1.348, 1.473), L_2=(-2.096, 0.03881), L_3=(-0.2338, 2.006), L_4=(-1.035, -1.647), L_5=(1.773, 0.5767), L_6=(0.961, -1.875), L_7=(0.3455, -0.6233), L_8=(-0.6786, -0.01292), L_9=(-0.01654, 0.5457). Following the procedure discuss in case 1 to discuss stability.

Lagrange Points	Eigenvalues	Stability
L_1	$\pm(-0.419894 + 0.789047i), \pm(0.419894 + 0.789047i)$	Unstable
L_2	$\pm 1.16815i, \pm 0.835508$	Unstable
L_3	$\pm 1.14394i, \mp 0.778688$	Unstable
L_4	$\pm(-0.419894 + 0.789047i), \pm(0.419894 + 0.789047i)$	Unstable
L_5	$\pm(0.412667 + 0.813329i), \pm(-0.412667 + 0.813329i)$	Unstable
L_6	$\pm 1.21392i, \mp 0.910721$	Unstable
L_7	$\mp 10.1277, \pm 7.22954i$	Unstable
L_8	$\mp 9.06969, \pm 6.41843i$	Unstable
L_9	$\mp 9.36297, \pm 6.64439i$	Unstable

TABLE 4.2: Stability Analysis Case 2 : $a = 0.9$, $b = -0.1$, c_1 = -0.52, $c_2 = 0.88$.

Case 3

By taking $a = 1.5$, $b = 0.4$, c_1 = -0.96, $c_2 = 0.99999$ and Lagrange points are L_1=(0.26, -1.3), L_2=(-0.85, 0.12), L_3=(-1.31, 1.87), L_4=(-0.601, 0.8147), L_5=(-0.05, 1.19). Following the procedure discuss in case 1 to discuss stability.

Lagrange Points	Eigenvalues	Stability
L_1	$\pm(-0.328945 + 0.857394i)$, $\pm(0.328945 + 0.857394i)$	Unstable
L_2	∓ 7.33541, $\pm 5.04489i$	Unstable
L_3	$\pm 1.23901i$, ∓ 1.20155	Unstable
L_4	∓ 6.78128, $\pm 4.77528i$	Unstable
L_5	∓ 6.52664, $\pm 4.50241i$	Unstable

TABLE 4.3: Stability Analysis Case 3: $a = 1.5$, $b = 0.4$, c_1 = -0.96, $c_2 = 0.99999$.

Case 4

By taking $a = 1.5$, $b = 0.4$, $c_1 = 1.05$, $c_2 = 0.13$ and Lagrange points are L_1(0.01602, 2.376), L_2(-0.004887, 1.183), L_3(0.7131, 0.2378), L_4(-0.681, 0.1432), L_5(0.05785, -1.595).

Following the procedure discuss in case 1 to discuss stability.

Lagrange Points	Eigenvalues	Stability
L_1(0.01602, 2.376)	$\pm(-0.641178 + 0.327483i)$, $\pm(0.641178 + 0.327483i)$	Unstable
L_2(-0.004887, 1.183)	∓ 7.54957, $\pm 0.619844i$	Unstable
L_3(0.7131, 0.2378)	$\pm 7.49621i$, ± 0.831828	Unstable
L_4(-0.681, 0.1432)	∓ 7.32335, $\pm 6.16001i$	Unstable
L_5(0.05785, -1.595)	$\pm 1.31857i$, ∓ 0.324714	Unstable

TABLE 4.4: Stability Analysis Case 4: $a = 1.5$, $b = 0.4$, $c_1 = 1.05$, $c_2 = 0.13$.

4.1.1 Newton Basins of Attraction

The Newton-Raphson method is a widely-used numerical technique for iteratively approximating roots of nonlinear equations. In our analysis of equilibrium points, we utilize the Newton-Raphson method to assess the basins of attraction. This method proves effective in determining the convergence of trajectories originating from the neighborhood of an equilibrium point. Our focus is on fixed-point basin of attraction, signifying that a set of points progressively converges, under successive transformations, towards Lagrange point. This technique is applicable to multivariate function systems, allowing for the iterative solution of equations of the form $f(x) = 0$.

$$x_{n+1} = x_n - J^{-1} f(x_n).$$

In the given iterative scheme, where $f(x_n)$ represents the equations and J^{-1} is the inverse Jacobian matrix, the process can be decomposed for each set of coordinates (x, y) as follows:

$$x_{n+1} = x_n - \left(\frac{\Omega_x \Omega_{yy} - \Omega_y \Omega_{xy}}{\Omega_{yy}\Omega_{xx} - \Omega_{xy}^2} \right)_{(x_n, y_n)}, \tag{4.18}$$

$$y_{n+1} = y_n + \left(\frac{\Omega_x \Omega_{yx} - \Omega_y \Omega_{xx}}{\Omega_{yy}\Omega_{xx} - \Omega_{xy}^2} \right)_{(x_n, y_n)}. \tag{4.19}$$

At the n^th point in the iterative process, x_n and y_n represent the coordinate values of x and y, respectively.

The subscripts indicate the corresponding first and second-order partial derivatives of the effective potential function $\Omega(x,\, y)$. The equations governing the effective potential, as given in equation (4.8) are:

$$\Omega(x,y) = \frac{x^2+y^2}{2} + \left[\frac{m_0}{\sqrt{x^2+(y-b)^2}} + \frac{m_1}{\sqrt{(x+1)^2+y^2}} \right] + \left[\frac{m_2}{\sqrt{x^2+(y-a)^2}} + \frac{m_3}{\sqrt{(x-c_1)^2+(y-c_2)^2}} \right], \tag{4.20}$$

where the mutual distances are defined as follows:

$$\begin{aligned} r_{40} &= \sqrt{x^2 + (y-b)^2}, \\ r_{41} &= \sqrt{(x+1)^2 + y^2}, \\ r_{42} &= \sqrt{x^2 + (y-a)^2}, \\ r_{43} &= \sqrt{(x-c_1)^2 + (y-c_2)^2}. \end{aligned}$$

The underlying principle of the Newton-Raphson method is as follows:
begin with an initial condition (x, y) that initiates the computation on the configuration plane. If the starting point rapidly converges to one of the equilibrium points, then this particular point (x, y) becomes part of the root's convergence. Once the successive approximations converge to an attractor, the iterative process is stoped.

4.1.2 Case 1 : Basins of Attraction for Five Lagrange Points

Choosing any initial condition for (x, y) and solving equation (4.17), one can reached the Lagrange point like if we take initial condition from the red region then we reach the L_2.

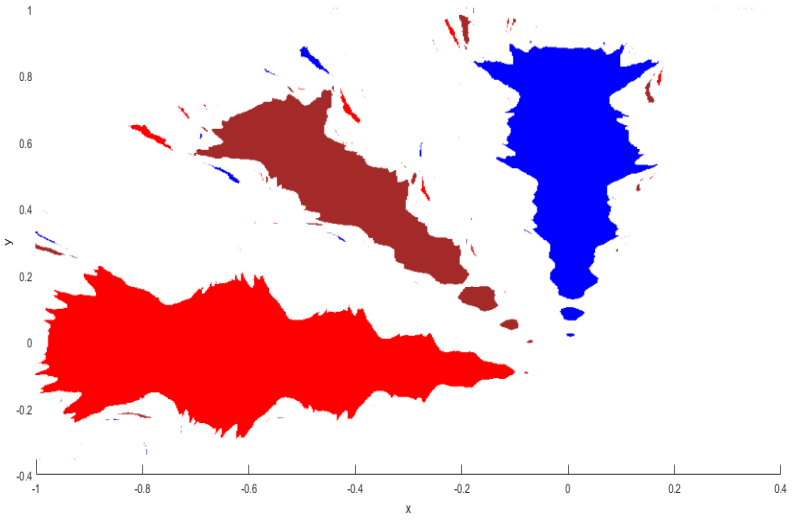

FIGURE 4.14: Case 1: Newton basins of attraction in xy configuration plane, where $a = 0.9$, $b = -0.1$, $c_1 =$ -0.61, $c_2 = 0.71$. Initial conditions leading to specific equilibrium points are marked with distinct colors: L_1 ('Brown'), L_2 ('Red'), L_3 ('Blue'), L_4 ('Magenta'), L_5 ('Dark Red').

4.1.3 Case 2 : Basins of Attraction for Nine Lagrange Points

Due to colour visibility, we show two picture of case 2 with different range.

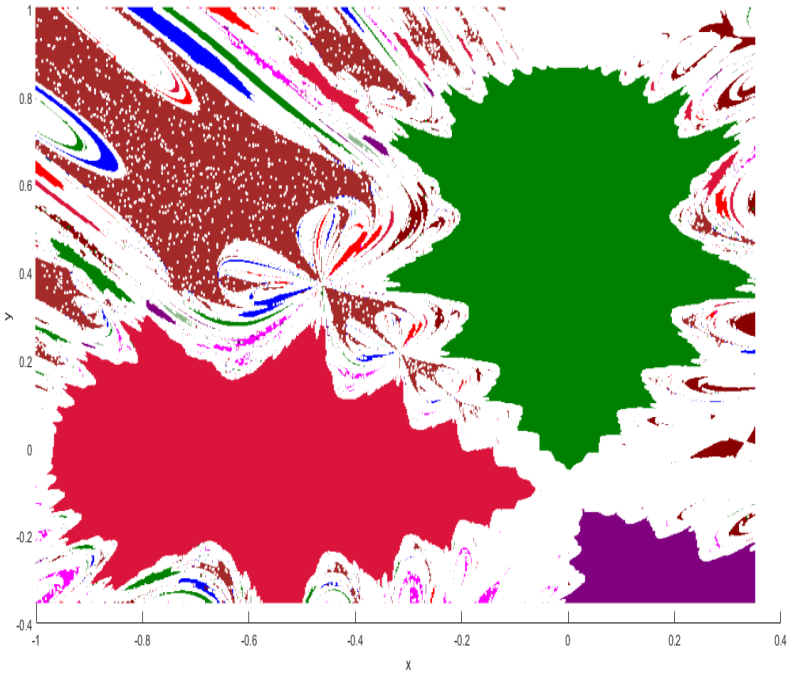

FIGURE 4.15: Case 2(a): Newton basins of attraction in xy configuration plane, where $a = 0.9$, $b = -0.1$, $c_1 = 0.52$, $c_2 =$ -0.88. Initial conditions leading to specific equilibrium points are marked with distinct colors: L_1 ('Brown'), L_2 ('Red'), L_3 ('Blue'), L_4 ('Magenta'), L_5 ('Khaki'), L_6 ('DarkSeaGreen'), L_7 ('Purple'), L_8 ('Crimson'), L_9 ('Green').

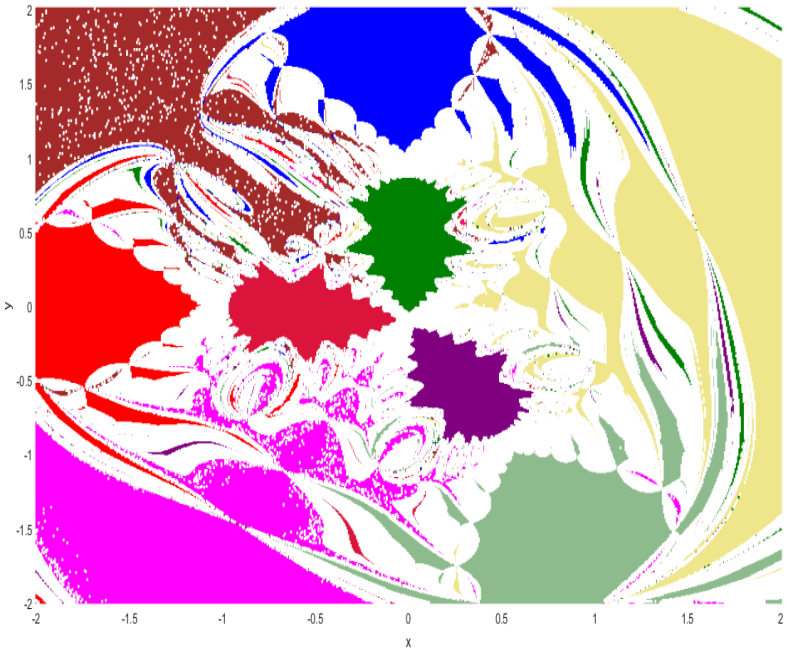

FIGURE 4.16: Case 2(b): Newton basins of attraction in xy configuration plane, where $a = 0.9$, $b = -0.1$, $c_1 = 0.52$, $c_2 =$ -0.88. Initial conditions leading to specific equilibrium points are marked with distinct colors: L_1 ('Brown'), L_2 ('Red'), L_3 ('Blue'), L_4 ('Magenta'), L_5 ('Khaki'), L_6 ('DarkSeaGreen'), L_7 ('Purple'), L_8 ('Crimson'), L_9 ('Green').

4.1.4 Case 3 : Basins of Attraction for Five Lagrange Points

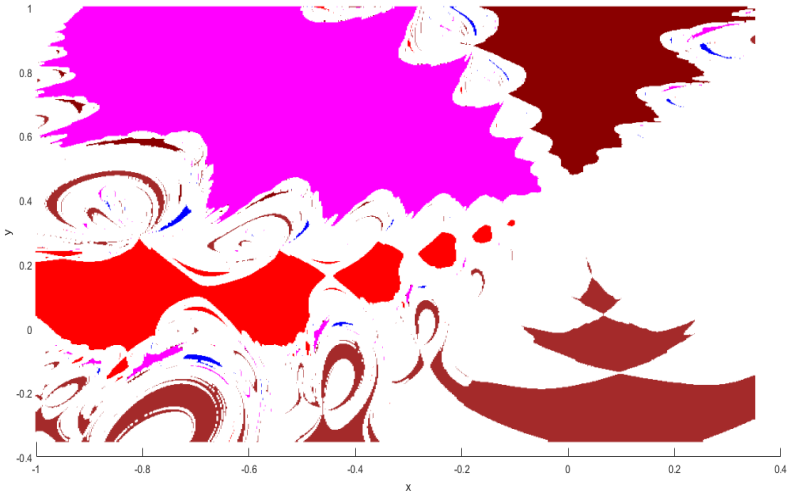

FIGURE 4.17: Case 3: Newton basins of attraction in xy configuration plane, where $a = 1.5$, $b = 0.4$, c_1 = -0.96, $c_2 = 0.9999$. Initial conditions leading to specific equilibrium points are marked with distinct colors: L_1 ('Brown'), L_2 ('Red'), L_3 ('Blue'), L_4 ('Magenta'), L_5 ('Dark Red').

4.1.5 Case 4 : Basins of Attraction for Five Lagrange Points

Due to colour visibility, we take three picture of case 4 with different range.

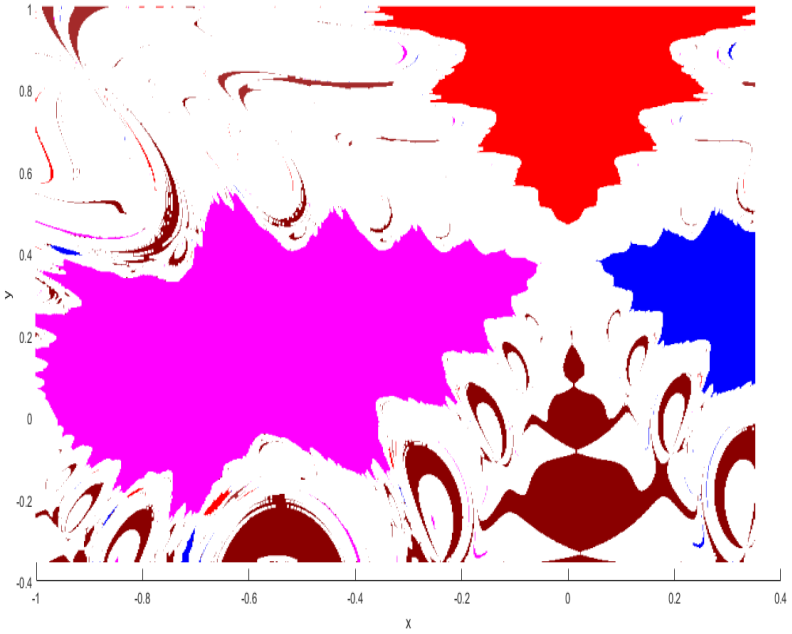

FIGURE 4.18: Case 4 (a): Newton basins of attraction in xy configuration plane, where $a = 1.5$, $b = 0.4$, $c_1 = 1.05$, $c_2 = 0.13$. Initial conditions leading to specific equilibrium points are marked with distinct colors: L_1 ('Brown'), L_2 ('Red'), L_3 ('Blue'), L_4 ('Magenta'), L_5 ('Dark Red').

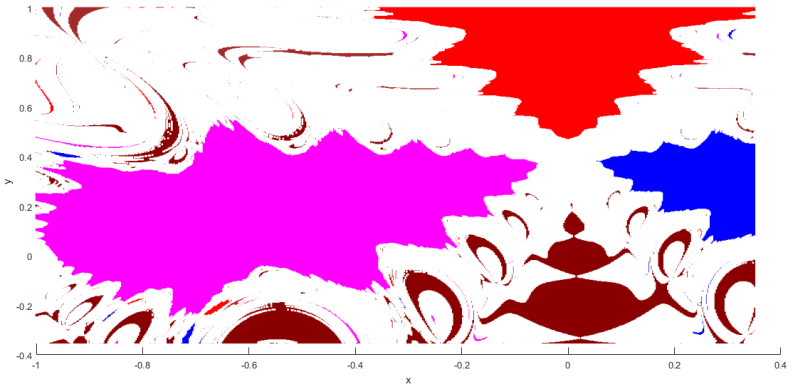

FIGURE 4.19: Case 4(b): Newton basins of attraction in xy configuration plane, where $a = 1.5$, $b = 0.4$, $c_1 = 1.05$, $c_2 = 0.13$. Initial conditions leading to specific equilibrium points are marked with distinct colors: L_1 ('Brown'), L_2 ('Red'), L_3 ('Blue'), L_4 ('Magenta'), L_5 ('Dark Red').

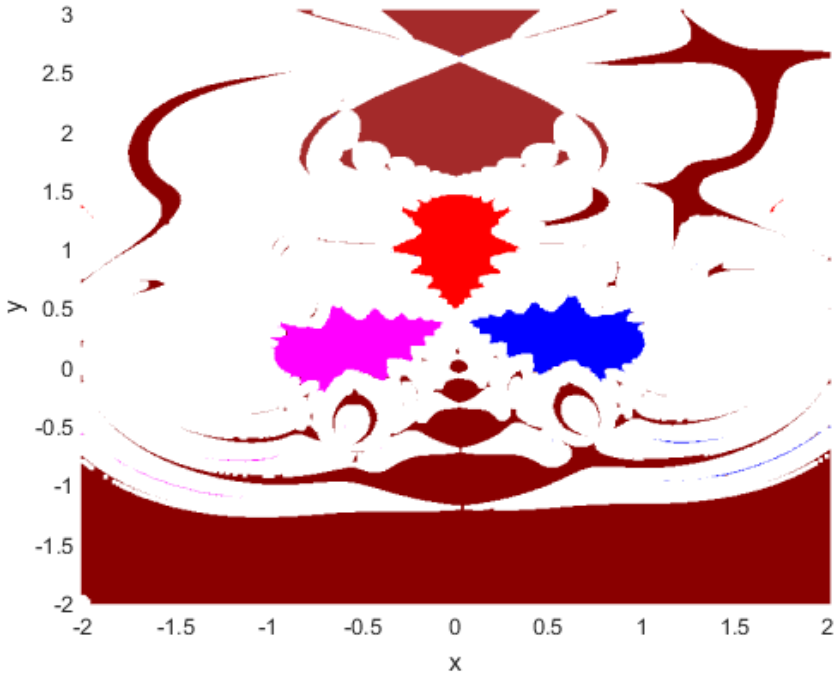

FIGURE 4.20: Case 4(c): Newton basins of attraction in xy configuration plane, where $a = 1.5$, $b = 0.4$, $c_1 = 1.05$, $c_2 = 0.13$. Initial conditions leading to specific equilibrium points are marked with distinct colors: L_1 ('Brown'), L_2 ('Red'), L_3 ('Blue'), L_4 ('Magenta'), L_5 ('Dark Red').

Chapter 5

Conclusions

In this research, we utilize Shoaib [2] research paper, his discussion centers on Central Configurations (CC) in the $4B$ problem with varying masses. Shoaib identifies both convex and concave CC by employing two distinct cases. In these cases, we introduce a fifth primary body as a restricted body, and find its trajectory around the primary masses. We generate Contour plots to visualize the paths, and find Lagrange points and their stability. Additionally, we determine the Basin of Attraction for these Lagrange points. we investigated the movement of a small mass m_4 in the xy-plane, influenced by the gravitational forces of four primary masses (m_0, m_1, m_2 and m_3). Four different masses form the vertices of an convex and concave central configuration as they move. After establishing the equation of motion for m_4, considering its negligible mass and minimal impact on the four primaries, we calculated equilibrium point positions across various intervals. We assessed the stability of these points by determining eigenvalues using Mathematica.

The parameters in the equation of motion influenced the positions of these equilibrium points. Numerical analysis indicated that all identified equilibrium points in the xy-plane are unstable. Another aspect of our study involves employing the multivariate version of the Newton-Raphson iterative method to examine the basins of convergence towards the liberation points of the dynamical system. We plotted the Newton-Raphson basins of attraction in the xy-plane. The shape, nature, and number of equilibrium points exhibited significant variation with changes in the positions of the primaries. These

attracting domains play a crucial role in explaining how the system liberation points attract each point in the configuration plane, acting as attractors.

Bibliography

[1] G. Smith, "Newton's philosophiae naturalis principia mathematica," 2007.

[2] M. Shoaib, B. Benhammouda, B. A. Steves, and W. L. Sweatman, "Central configurations in the general four body coplanar problem with different masses," 2023.

[3] F. R. Moulton, "On a class of particular solutions of the problem of four bodies," *Transactions of the American Mathematical Society*, vol. 1, no. 1, pp. 17–29, 1900.

[4] J. I. Palmore, "Measure of degenerate relative equilibria. i," *Annals of Mathematics*, vol. 104, no. 3, pp. 421–429, 1976.

[5] J. Casasayas, "Dimensions of the invariant manifolds associated with equilibrium points in the n-body problem," in *Applications of Modern Dynamics to Celestial Mechanics and Astrodynamics: Proceedings of the NATO Advanced Study Institute held at Cortina d'Ampezzo, Italy, August 2–14, 1981*, pp. 337–337, Springer, 1982.

[6] G. L. Ross, D. S. Soutar, D. Gordon MacDonald, T. Shoaib, I. Camilleri, A. G. Roberton, J. A. Sorensen, J. Thomsen, P. Grupe, J. Alvarez, *et al.*, "Sentinel node biopsy in head and neck cancer: preliminary results of a multicenter trial," *Annals of surgical oncology*, vol. 11, pp. 690–696, 2004.

[7] Q. Liu, H. Fu, F. Sun, H. Zhang, Y. Tie, J. Zhu, R. Xing, Z. Sun, and X. Zheng, "mir-16 family induces cell cycle arrest by regulating multiple cell cycle genes," *Nucleic acids research*, vol. 36, no. 16, pp. 5391–5404, 2008.

[8] A. Kirste, B. Elsler, G. Schnakenburg, and S. R. Waldvogel, "Efficient anodic and direct phenol-arene c, c cross-coupling: The benign role of water or methanol," *Journal of the American Chemical Society*, vol. 134, no. 7, pp. 3571–3576, 2012.

[9] B. Érdi and Z. Czirják, "Central configurations of four bodies with an axis of symmetry," *Celestial Mechanics and Dynamical Astronomy*, vol. 125, pp. 33–70, 2016.

[10] M. Shoaib, A. R. Kashif, and I. Szücs-Csillik, "On the planar central configurations of rhomboidal and triangular four-and five-body problems," *Astrophysics and Space Science*, vol. 362, no. 10, p. 182, 2017.

[11] C. Reigber, R. Schmidt, F. Flechtner, R. König, U. Meyer, K.-H. Neumayer, P. Schwintzer, and S. Y. Zhu, "An earth gravity field model complete to degree and order 150 from grace: Eigen-grace02s," *Journal of Geodynamics*, vol. 39, no. 1, pp. 1–10, 2005.

[12] M. Corbera, J. M. Cors, and G. E. Roberts, "A four-body convex central configuration with perpendicular diagonals is necessarily a kite," *Qualitative theory of dynamical systems*, vol. 17, pp. 367–374, 2018.

[13] H. Álvarez, A. Mariño, N. Valcarce, J. García-González, H. Díaz-Cambre, and J. M. Llibre, "Overdose of elvitegravir/cobicistat/emtricitabine/tenofovir alafenamide in an hiv-1-infected subject with attempted suicide," *Infection*, vol. 47, pp. 115–119, 2019.

[14] J. Wang, J.-Y. Yang, I. M. Fazal, N. Ahmed, Y. Yan, H. Huang, Y. Ren, Y. Yue, S. Dolinar, and M. Tur, "Terabit free-space data transmission employing orbital angular momentum multiplexing," *Nature photonics*, vol. 6, no. 7, pp. 488–496, 2012.

[15] R. P. Ishii and R. F. de Mello, "An online data access prediction and optimization approach for distributed systems," *IEEE transactions on parallel and distributed systems*, vol. 23, no. 6, pp. 1017–1029, 2011.

[16] E. Perez-Chavela and M. Santoprete, "Convex four-body central configurations with some equal masses," *Archive for rational mechanics and analysis*, vol. 185, pp. 481–494, 2007.

[17] J. Bernat, J. Llibre, and E. Perez-Chavela, "On the planar central configurations of the 4-body problem with three equal masses," *preprint*, vol. 1, pp. 105–112, 2009.

[18] M. Santoprete and F. Xu, "Global stability in a mathematical model of deradicalization," *Physica A: statistical mechanics and its applications*, vol. 509, pp. 151–161, 2018.

[19] M. Celli, "The central configurations of four masses x,- x, y,- y," *Journal of Differential Equations*, vol. 235, no. 2, pp. 668–682, 2007.

[20] M. Corbera and J. Llibre, "Central configurations of the 4-body problem with masses $m_1 = m_2 > m_3 = m_4 =$ m> 0 and m small," *Applied Mathematics and Computation*, vol. 246, pp. 121–147, 2014.

[21] L. Xia, K. B. Monroe, and J. L. Cox, "The price is unfair! a conceptual framework of price fairness perceptions," *Journal of marketing*, vol. 68, no. 4, pp. 1–15, 2004.

[22] W. MacMillan and W. Bartky, "Permanent configurations in the problem of four bodies," *Transactions of the American Mathematical Society*, vol. 34, no. 4, pp. 838–875, 1932.

[23] M. Corbera, J. M. Cors, J. Llibre, and E. Pérez-Chavela, "Trapezoid central configurations," *Applied Mathematics and Computation*, vol. 346, pp. 127–142, 2019.

[24] J. M. Cors and G. E. Roberts, "Four-body co-circular central configurations," *Nonlinearity*, vol. 25, no. 2, p. 343, 2012.

[25] L. Bakker and S. Simmons, "A separating surface for sitnikov-like n+ 1-body problems," *Journal of Differential Equations*, vol. 258, no. 9, pp. 3063–3087, 2015.

[26] P. Rodgers, *Nanoscience and technology: a collection of reviews from nature journals*. World Scientific, 2009.

[27] W. L. Hamilton, J. Leskovec, and D. Jurafsky, "Diachronic word embeddings reveal statistical laws of semantic change," *arXiv preprint arXiv:1605.09096*, 2016.

[28] E. E. Zotos, "Fractal basins of attraction in the planar circular restricted three-body problem with oblateness and radiation pressure," *Astrophysics and Space Science*, vol. 361, no. 6, p. 181, 2016.

[29] M. S. Suraj, R. Aggarwal, K. Shalini, and M. C. Asique, "Out-of-plane equilibrium points and regions of motion in the photogravitational r3bp when the primaries are heterogeneous spheroid with three layers," *New Astronomy*, vol. 63, pp. 15–26, 2018.

[30] M. S. Suraj, E. I. Abouelmagd, R. Aggarwal, and A. Mittal, "The analysis of restricted five–body problem within frame of variable mass," *New Astronomy*, vol. 70, pp. 12–21, 2019.

[31] E. E. Zotos and M. Sanam Suraj, "Basins of attraction of equilibrium points in the planar circular restricted five-body problem," *Astrophysics and Space Science*, vol. 363, pp. 1–16, 2018.

[32] B. I. Epureanu and H. S. Greenside, "Fractal basins of attraction associated with a damped newton's method," *SIAM review*, pp. 102–109, 1998.

[33] M. S. Suraj, P. Sachan, E. E. Zotos, A. Mittal, and R. Aggarwal, "On the newton-raphson basins of convergence associated with the libration points in the axisymmetric five-body problem: the concave configuration," *arXiv preprint arXiv:1904.04618*, 2019.

[34] M. R. Spiegel and Y. Proykova, "Schaum's outline of theory and problems of theoretical mechanics: with an introduction to lagrange's equations and hamiltonian theory," 1967.

[35] S. Alrasheed, *Principles of mechanics: Fundamental university physics*. Springer Nature, 2019.

[36] R. Moeckel, "Central configurations," *Central Configurations, Periodic Orbits, and Hamiltonian Systems, Adv. Courses Math. CRM Barcelona, Birkhäuser/Springer, Basel*, pp. 105–167, 2015.

[37] A. E. Roy, *Orbital motion*. CRC Press, 2020.

[38] W. H. Goodyear, "Completely general closed-form solution for coordinates and partial derivative of the two-body problem," *Astronomical Journal, Vol. 70, p. 189*, vol. 70, p. 189, 1965.